IMAGE ENHANCEMENT USING DIGITAL ADAPTIVE FILTERING

by

PAUL JOSEPH CURLANDER

B.S., University of Colorado
1974

SUBMITTED IN PARTIAL FULFILLMENT
OF THE REQUIREMENTS FOR THE
DEGREE OF

MASTER OF SCIENCE

at the

MASSACHUSETTS INSTITUTE OF TECHNOLOGY

August, 1977

Signature of Author .....
Department of Electrical Engineering,
August 12, 1977

Certified by .....
Thesis Supervisor

Accepted by .....
Chairman, Departmental Committee on Graduate Students

IMAGE ENHANCEMENT USING DIGITAL ADAPTIVE FILTERING

by

PAUL JOSEPH CURLANDER

Submitted to the Department of Electrical Engineering on August 12, 1977 in partial fulfillment of the requirements for the Degree of Master of Science.

ABSTRACT

Image enhancement is an attempt to improve the aesthetic qualities of an image. Improvement of these qualities makes the image subjectively better. Adding overshoot to edges sharpens an image. Sharper images are judged to be subjectively better until sharpening results in light and dark band artifacts on edges. Considerations of human perception of brightness and contrast led to this experimentation with adaptive filtering to improve sharpness and minimize artifacts. A computer program has been developed which sharpens digitized pictures according to local area brightness and contrast content. By balancing sharpening between low and high contrast edges and dark and light tones, sharper pictures without artifacts are produced. Comparison pictures using linear, homomorphic, and previous adaptive filtering algorithms are also shown. Another application of adaptive filtering is noise suppression. A noisy picture is smoothed, eliminating the noise, then adaptively filtered to recover the edges and enhance the detail.

Preliminary subjective testing to determine optimum

overshoot height as a function of brightness and contrast is also reported. Optimum height gives maximum sharpening without artifacts. The results show that optimum overshoot height is an increasing function of both brightness and contrast. As a function of brightness, optimum overshoot follows a power law form. This implies that nonlinear perception of brightness follows a power law form.

Thesis Supervisor: William F. Schreiber
Title: Professor of Electrical Engineering

ACKNOWLEDGEMENTS

I wish to thank Professor William F. Schreiber for suggesting this work and for his helpful advice throughout this project. I also wish to thank John Ratzel and Ulick Malone for their invaluable assistance in helping me to learn the PDP 11/40 software system.

Paul Curlander

August 12, 1977

TABLE OF CONTENTS

TABLE OF FIGURES

TABLE OF FIGURES (continued)

* EAF= Equalized Adaptive Filtering

IMAGE PROCESSING BACKGROUND AND PROBLEM STATEMENT

This thesis details an investigation of image enhancement by adaptive, picture dependent techniques. From the original picture a linearly high passed "edge" picture is derived. This edge picture is then scaled pel (picture element) by pel according to the local brightness and spatial frequency (contrast) content and added back to the original. Previous work in adaptive picture processing indicates that pictures subjectively better than those produced by picture independent techniques are possible. However, deformation of high contrast edges was an unfortunate by-product of this processing. In light of this earlier work two questions arise. First, can a frequency or contrast measure be found that will avoid the deformation of edges? The research presented here will show that it can. Secondly, by modifying the scaling function is it possible to obtain subjectively better pictures than were previously obtained by adaptive processing? Again, these results show that better pictures are indeed achievable. In the context of this work, subjectively better is taken to mean an improvement in the aesthetic qualities of a picture as seen by a human observer.

Image enhancement is an attempt to subjectively improve the appearance of an image and to present additional information to the viewer. Processing for quality improvement is distinct from image restoration operations. The latter arises due to some serious degradation in the imaging process and may be

corrected if specific information about the degradation is available (1), (2), (3), (4). The former assumes the existence of a good image and its goal is to improve the subjective appearance until unnatural artifacts due to this processing start to appear. These techniques are normally based on knowledge of the important aspects of picture quality and human visual characteristics.

Three important elements of picture quality are contrast, dynamic range, and sharpness (5). Contrast is important to depth perception and detail detection. Low contrast between objects in a photograph causes the picture to look flat. High contrast makes small objects easier to distinguish from the background and aids in conveying the depth information of the picture. The contrast of the image depends on the dynamic range of the reproduction media. This is the total range of available brightnesses and is given by the ratio of the reflectance of the lightest and darkest regions. Therefore, to enhance the detail of the picture, the contrast should be as high as possible which means the dynamic range should be as large as possible.

It has long been known that adding overshoot to edges makes them appear sharper (6), (7). Sharper pictures are judged to be subjectively better until sharpening results in undesirable light and dark band artifacts on edges (8). The nonlinearity of human vision indicates that minimal artifacts and maximum sharpening will not be achieved using symmetric overshoot

and undershoot. Artifact visibility is due to the contrast sensitivity of human vision. Psychovisual experimentation measuring the just noticeable brightness difference as a function of brightness indicates that contrast sensitivity decreases as brightness increases (9). In terms of edge shaping this means that smaller undershoot and relatively larger overshoot will be required to minimize artifacts and maximize sharpening. Experimentation to measure the just noticeable brightness difference in a test field superimposed on a background field indicates that contrast sensitivity decreases as the brightness difference between the test field and background increases (10). Therefore, it is to be expected that as the magnitude of the edge increases, greater overshoot and undershoot for a given brightness level will be allowed without producing artifacts.

While contrast and sharpness are important contributors to image quality, pictoral noise is a significant detriment. The nonlinearity discussion above indicates that noise should be more visible in the darker tones because all increments are more visible there. Experimental evidence shows that this is true (11), (12). Mitchell (13) found that wide band noise is most visible in the four to six cycle per degree (cpd) range. When noise is present in a picture its visibility is decreased and is least visible in picture areas having similar frequency content. Since picture detail and contours will lie in this four to six cpd range, this indicates that noise will be most visible in the dark low frequency parts of the picture. Texture

consists of areas of roughly constant brightness and point to point changes in reflectance. The way in which the visual system perceives texture is not completely clear. If in the sharpening process the texture areas are accentuated too much, their appearance becomes unnatural and detracts from the quality of the picture.

From the preceding discussion it is clear that in image enhancement for quality improvement several things are desirable. First, edges should be sharpened as much as possible. The optimal shaping is such that as the sharpening is increased, low and high contrast detail in both the highlights and the lowlights of the picture should improve until light and dark band artifacts start appearing simultaneously. Secondly, contrast and dynamic range should be as large as possible. The dynamic range is limited by the output media. However, sharpening edge transitions leads to subjectively increased contrast (9), (19) and thus contrast enhancement can be expected from the sharpening process. Thirdly, picture noise must not be amplified especially in the dark constant parts of the picture. Lastly, the texture areas should not appear unnatural as a result of the processing.

Several techniques have been used to implement parts of this desired enhancement. Linear high pass filtering is often used for sharpening pictures (14). This adds symmetric overshoot to edges and the amount of overshoot depends on the contrast of the edge. This has several disadvantages. As noted above, minimum artifacts and maximum sharpening cannot be

achieved using symmetric shaping. As the sharpening is turned up, artifacts on high contrast edges will become visible. If sharpening is stopped when these artifacts start to appear, the low contrast edges will be far from maximally sharpened. Another problem in adding large overshoot and undershoot to the high contrast edges is a possibility of exceeding the allowable brightness values. The allowable brightness range is set by the internal computer representation (i.e., all pel values must be between 0 and 255) and by the picture media. Unless the tone scale of the picture is compressed, some parts of the output may try to be "blacker than black" or "whiter than white."

The homomorphic filtering concept describes pictures as being composed of two multiplicative components, the illumination and the reflectance (15), (16). By taking the logarithm of the image it may be separated into additive components. These components may then be processed independently with the assumption that the illumination comprises the low frequency range and the reflectance lies in the high frequency range. Assuming this is true, to more uniformly illuminate the picture, linear high pass filtering of the logarithm with a dc gain less than one is done to decrease the illumination component and emphasize the reflectance component. This filtering is followed by an antilog transformation. Although the validity of this reasoning is in doubt (17), picture quality improvement exceeding linearly filtered pictures has been achieved.

The high pass filtering places symmetric overshoot on the edges of the logarithm pictures. The antilog transform then results in greater peaks on the brighter edges. The size of these peaks is dependent on the contrast of the edge, the brightness level, and the antilog transform. This shaping is more consistent with the nonlinear characteristics of the eye as pointed out earlier. However, artifacts are readily visible on the high contrast edges. Dark bands are sharply reduced but the light bands are still present and more visible than in linearly filtered pictures. Because of the antilog operation there is no danger of falling below the lower limit of internal computer pel values of zero. There is no guarantee of remaining below the upper limit on internal value or within either limit of the output media dynamic range (17). In addition, the dc gain of less than one changes the tone scale and decreases macro area contrast, particularly in the highlights. For pictures whose dynamic range greatly exceeds the available range this may be acceptable, but in general, reducing the dynamic range is not desirable.

Realizing that picture independent filtering adds far too much overshoot to the high contrast edges, Gilkes (18) tried an adaptive filtering scheme. A low passed version of the picture was subtracted from the original to obtain an edge picture. The idea was to scale the edge signal before adding it back to the original. High contrast edges could be scaled down and low contrast edges could be scaled up to make sharpening

more even. Brightness was also a factor in his scaling. Taking into account the decreased contrast sensitivity in the highlights of the picture, edge height was increased linearly with brightness. His brightness measure was the pel value from the low pass filtered picture. His contrast measure was the pel value from the edge picture. Picture quality better than that provided by linear and homomorphic filtering was achieved. Specifically, the light band artifacts on high contrast edges were significantly reduced. The effect of linear filtering, homomorphic filtering and Gilkes' adaptive filtering on a sample edge, and details of these three processing techniques, are given in Appendix I.

There are several disadvantages to Gilkes' filtering process. The edge picture varys from pel to pel because it is the high frequency component of the original picture. Using these values as a contrast measure leads to distortion of the edge shape which is very undesirable. Using the low pass pel value as a brightness measure causes the overshoot and undershoot heights to be equal. This was noted previously as not being optimum. Inspection of Gilkes' pictures also shows that low contrast edges and detail could have been sharpened even more.

This research was undertaken to subjectively optimize the adaptive filtering scheme implemented by Gilkes. The goal is to equalize and maximize the sharpening without artifacts and without distorting the shape of the edge. By properly

balancing the sharpening of low, medium, and high contrast edges, sharper and subjectively better pictures should be possible. The experimental results of Chapter III show that this is indeed true.

In scaling the edge picture there are two considerations, brightness and contrast. The quantities to be optimized are the brightness and contrast scaling functions. It seems appropriate to separate the functions and study them individually.

Contrast sensitivity measurements as a function of brightness should give some insight to the desired overshoot height as a function of brightness. The most well known result is the Weber-Fechner law which indicates contrast sensitivity is proportional to brightness (9). Using the assumption that just noticeable brightness differences result in equal increments of perceived brightness independent of the brightness level, nonlinear brightness perception could then be modelled as a logarithmic detector. Related work which also depends on the eye's contrast sensitivity has been done on minimizing the visibility of quantization contours and pseudo-random noise (10), (11), (12), (17). These results indicate that a power law or modified logarithm are a better fit to the eye's nonlinear behavior than the logarithmic detector.

Using the above assumption that the just noticeable difference in brightness results in equal increments in perceived brightness for all levels, the reverse derivation can be carried out and the contrast sensitivity functions for the power law

and modified logarithm may be determined. Appendix II contains the derivation of these functions for a dynamic range of 1.6 log units corresponding to the output media to be used. Because of the questionable validity of this assumption (8) and because of the different viewing situation involved in edge artifacts, this investigator undertook to measure desired overshoot height as a function of brightness. These experiments and the results are described in Chapter II.

Desirable overshoot height for a given brightness will increase as the magnitude of the edge increases. However, when linear filtering is used to derive the edge picture, it gives too much undershoot on the dark side and too little overshoot on the light side, as seen by inspecting linearly filtered pictures. Because no quantitative data existed it was decided to make subjective measurements of desired overshoot height as a function of edge magnitude (contrast). These results are also reported in Chapter II.

Once the overshoot height as a function of brightness and edge magnitude is known, it remains to implement this knowledge as scaling functions in the adaptive filtering process. Because linear filtering produces edge heights independent of brightness, the brightness scaling should be straightforward. It should differ only by a proportionality factor from the overshoot versus brightness curve. The brightness measure should be the full spectrum (original) pel value in order to avoid making the overshoot and undershoot heights equal as results when the low passed pel value is used.

The contrast scaling function is not as straightforward. The contrast measure must be approximately constant over the entire edge or else the shape of the edge will be distorted. Taking the absolute value of the magnitude of the gradient of an image will produce a new image in which all the edges and detail are present. All constant tone areas will be blacked out. It was hoped that by adequately smoothing this gradient a relatively constant contrast measure could be formed.

The contrast scaling function must take into account the contrast measure, the effect of the linear filter (edge height proportional to contrast), and the desired overshoot height as a function of contrast. It is not obvious how the contrast scaling function can be adequately determined other than by the sequence of processing, visual evaluation, and subsequent refinement. This evaluation must also take into account the effect of the processing on texture areas. The sharpening of texture must be acceptable. A description of this experimentation and its results are given in Chapter III.

SUBJECTIVE EXPERIMENTATION TO DETERMINE OPTIMUM OVERSHOOT HEIGHT

This chapter describes the subjective testing to determine optimum overshoot height. Overshoot height was found to be an increasing function of both edge brightness and contrast. To determine the brightness dependency, nine measurements were made on very low contrast edges. The results are closely fitted by a power law function with an exponent between .3 and .5. To determine the contrast dependency, five measurements on edges of varying contrast were made for four different brightness ranges. The results indicate that desirable overshoot height increases nonlinearly with contrast. For edge magnitudes greater than twenty it is seen that linear filtering adds excessive overshoot height to edges.

A. SOFTWARE DESCRIPTION AND DISCUSSION

All image processing and experimentation was done on the Cognitive Information Processing Group's PDP 11/40 computer. Picture input and output to this system was done using the Laserphoto Facsimile Transmitter and Receiver. The pictures were scanned at a resolution of 111 lines per inch. A digital interface then sampled the scan line at 106 pels per inch. The samples were quantized to 8 bits per pel, taking on values in the range 0 to 255. In outputting the pictures, the digital data was reconverted to analog signals before being sent to the Laserphoto Receiver. This receiver used dry silver paper with a dynamic range of approximately 1.6 units or 40:1 brightness ratio.

All software required for input/output and picture storage already existed in CIPG's picture processing software system (20). A two dimensional convolution program used in the adaptive filtering experiments was also part of this software package. All programs specifically generated for this research were combined temporarily as part of the software system and could be called up when needed.

The objective of the subjective testing was to determine the desired overshoot and undershoot height as a function of brightness and contrast. The image used in the testing was a computer generated single dark stripe on a lighter background. It was decided to use such a picture because it was possible to observe the sharpening effect and any artifacts very easily and could be quickly compared to other similar pictures with varying degrees of sharpening.

When adaptive filtering is done the edge shaping will be generated by a linear filter. For this part of the experimentation it was important to know exactly the edge height and shape. It was decided to directly generate the overshoot and undershoot on the edge of the stripe instead of convolving the base picture with a sampled point spread function. Because the picture is one dimensional with only two edges, this addition of shaping to the edges is much faster than a convolution.

In order to sharpen pictures the overshoot and undershoot must roll off smoothly without any oscillation (6). Gilkes' experimentation showed that an edge width of ten pels was

approximately right for the resolution of the pictures which will eventually be processed. For these reasons, an exponential roll off with an edge width of roughly ten pels was chosen.

The input parameters to the program which generated the test picture were the stripe brightness, the background brightness, the overshoot height, and the undershoot height. The stripe and background brightness could be specified anywhere in the range 0 to 255 but the stripe brightness had to be less than or equal to the background brightness because undershoot was automatically added to the inside of the edge. The values of the exponential shaping for overshoot heights between zero and thirty were precomputed, rounded to the nearest integer, and stored in a table inside the program. When an overshoot height was specified, these values were called up and either added to or subtracted from the base picture depending on whether overshoot or undershoot was being generated. The integer exponential shapes used are tabulated in Appendix III.

To subjectively determine the optimum overshoot, observers had to compare the sharpening on a sequence of stripes. Informal preliminary tests indicated this was best accomplished by presenting the viewer with all edges simultaneously and with no more than six or seven choices. If edges were not viewed simultaneously, it was difficult to make any decision at all. If the pictures were viewed simultaneously but there were very many, again, the choice was difficult. As a result, it was decided to output all pictures to the Laserphoto

Receiver and construct a single page with a sequence of stripes for each edge measurement. An example of such a page is shown in Figure 1.

For each page the sharpening increases from left to right starting with the unsharpened picture. The increase in subjective contrast with sharpening is readily visible on these edges. In making these test pages, the objective was to have approximately six pictures which changed from the original with no sharpening to obviously too much with artifacts. The increase in sharpening between stripes was to be small but discernible, equally incremented, with about six pictures covering the entire range. Because artifact sensitivity is greater for dark, low contrast edges, it was to be expected that increments in overshoot would be smaller on these edges than the increments for high contrast, bright edges. All subjective qualities were the opinion of this investigator and it was hoped that other observers would select edges in the middle of the sharpness range. This would give the best accuracy.

Outputting these computer generated stripe pictures to the Laserphoto Receiver eventually proved to be a difficult process. If the picture was streaked in the region of the edge, it was useless. Many stripe pictures were output two or three times before acceptable pictures were obtained. Another problem encountered was the lack of a fixed relationship between internal pel values and output tones. If future research hopes to

increase the accuracy of the results presented here, these problems must be eliminated.

B. BRIGHTNESS MEASUREMENTS

The nine edges used to determine desired overshoot height as a function of brightness were low contrast edges. The brightness difference between the stripe and the background was 5 units on the internal scale of 0 to 255. A low contrast edge was used so that symmetric shaping could be applied. This simplified the generation of the pictures and reduced the dependency of the results on the definition of brightness. Brightness was defined to be the background brightness, but clearly on these very low contrast edges the difference is small. Overshoot measurements were taken at nine brightness levels. The edges used are listed in Figure 2. These measurements are separated by 20 units in the low and medium brightness range and gradually increase for the highlights where the curve can be expected to flatten out.

In adding overshoot and undershoot, the planned algorithm was to start with the original picture and add shaping symmetrically, incrementing the height by one for low tones, two for the middle tones, and three for the high tones. However, in the transition from internal pel values to the output media in order to preserve the goal of even increments of sharpening, slight variations were made. For example, on the 170-175 edge, the dark band artifacts seemed to exceed the light band artifacts

in limiting sharpening. The shaping was made slightly asymmetric to offset this. Figure 2 lists the edges and overshoot and undershoot heights used in the overshoot versus brightness measurements. A page of edges was constructed for each brightness measurement.

C. CONTRAST MEASUREMENTS

Gilkes' results indicated that only minimal sharpening was needed for edge magnitudes greater than 30. Because of this, measurements of overshoot height as a function of contrast were made for edges of 5, 10, 15, 20, and 30 for four different brightness ranges. A page of edges was made up for each measurement. Therefore, in each range five pages were made. With four brightness ranges, this required twenty pages in all. In each range the stripe brightness was held constant while the background was increased. The optimum overshoot for the background brightness was measured.

As before, it was desirable for the sharpening to increase evenly with six or seven pictures covering the range from no sharpening to oversharpened. The overshoot versus brightness measurements were all made with very low contrast edges so that symmetric shaping was appropriate. In these contrast measurements, this was no longer true. To keep light and dark band artifacts even, the overshoot and undershoot were symmetric on edges of 5 and 10, and asymmetric on edges of 15, 20, and 30. For edges of 15 and 20, overshoot exceeded undershoot height by one. For edges of 30, overshoot exceeded

undershoot height by two. Again, slight inconsistencies in the transition between internal computer values and output brightness caused some variation in these rules when this observer felt the artifacts were not coming up evenly. A list of edges used in the overshoot versus contrast measurement is given in Figure 3. Note that the four edges of contrast 5 were used in both the contrast and brightness tests.

D. TESTING PROCEDURE

Eight observers were used in the subjective experimentation. They were all MIT graduate students not involved in image processing work. All testing was done under office lighting conditions of approximately 65 foot candles of illumination. The prepared pages were laid in front of the subject on a desk. The subjects were all standing with a viewing distance of about 34 inches.

Before the measurements were started, the observer was shown a test sequence similar to the page in Figure 1. He was told that the pictures were sharper left to right. He was to pick the sharpest stripe without objectionable artifacts. He was shown which artifacts in the test sequence were considered to be objectionable. After this instruction, the pages were laid in front of him one at a time. The pages were randomly ordered in brightness and contrast. Because four pages were common to the brightness and contrast tests, a total of 25 pages were shown to each subject. No time limit was set for each decision, but the majority of answers came in less than ten

seconds. In general, the decisions seemed to be easy. The most difficult choices were for pages on which the increments in sharpness were not quite large enough. For example, the observers seemed to hesitate over the 210-215 edge and indicated that several pictures were acceptable. They were allowed to give only one answer.

E. SUBJECTIVE TESTING RESULTS

Results for all edges and all eight observers are tabulated in Appendix III. Approximately 84% of all answers were in the middle of the range of choices for each measurement. This was considered to be the most accurate range. In the few instances that observers picked the original as the only picture without artifacts, an interpolated value of one-half the second picture overshoot was used. This seemed reasonable because certainly some sharpening is desirable and a value of zero overshoot as optimum would clearly be wrong. For the case in which the largest possible overshoot was chosen, no interpolation was done. Perhaps the observer would have gone higher given the opportunity, but it was impossible to tell how much further.

For each edge measurement, out of the eight experimental values, the high and low value was eliminated and the remaining six values were averaged. For the overshoot versus contrast measurements, within each brightness group, the results were further smoothed by adding to each average the one from above

and below it and dividing by three. The endpoints of 5 and 30 were added to themselves and the next interior value, then divided by three. These operations are given in Appendix III. The results are tabulated in Figure 4.

For the overshoot versus brightness tests the low and the high value for each result was also eliminated. The remaining six values were averaged and then smoothed by the above process four times. This was done so a curve could be fitted to the results. The operations are given in Appendix III and the results are tabulated in Figure 5. Also listed is the internal brightness value and the reflection density of that brightness as determined by the Kodak Reflection Density Chart.

In order to compare the brightness results with the modified logarithm and power law predictions, the overshoot must be plotted against brightness on a 40:1 brightness scale. A 40:1 brightness ratio corresponds to 1.6 log units. On the Kodak Chart, the brighter values have a lower reflection density with a zero value assigned to white. Therefore:

$$B=10^{**}(1.6-D) \qquad 0 \leqslant D \leqslant 1.6, \quad 1 \leqslant B \leqslant 40$$

is the required conversion with a brightness of one the darkest tone and a brightness of forty the lightest tone. The symbol ** denotes exponentiation.

The overshoot as a function of brightness results are plotted in Figure 6 along with the predicted results from the power law and modified logarithm relationships as derived in

Appendix II. As expected, the desired overshoot height does increase with brightness and thus indicates asymmetric shaping is desirable. As a result of the smoothing, the middle and high brightness values are most accurate. The smoothing artificially increased the low brightness values because no value was available for the very dark tones.

In the middle and high tones, the results are fitted by the function 1.9(B**.3). However, the square root function is within 20% of these smoothed results. For measurements in which the increment in edge height between pictures is two, each result is accurate to within plus or minus one. For measured values of five, the margin of error is 20% and increases to 25% for measured values of four. Therefore, an exponential dependency of .5 appears to be within the experimental error. The modified logarithm prediction lies far below the measured values. These results indicate that the desired brightness function fits the power law form with an exponent between .3 and .5. This result can be used to infer the eye's nonlinear brightness perception function. Again, with the assumption that a just noticeable difference in brightness results in equal increments of perceived brightness for all levels, the eye's nonlinear perception function is a power law relationship with an exponent between .5 and .7.

The smoothed results of the overshoot versus contrast experiments are plotted versus contrast in Figure 7. As expected within each brightness range the acceptable overshoot increases with contrast. For all groups, the acceptable overshoot

at an edge magnitude of 30 is roughly twice that acceptable at an edge magnitude of 5. This is significant because the overshoot added by linear filtering is directly proportional to the edge magnitude. The overshoot added to an edge height of 30 would be six times greater than that added to an edge height of 5. The slope of the characteristic for linear filtering is approximately three times greater than it should be. For all brightness groups the overshoot height for an edge of 20 is between eight and ten. Linear filtering would add an edge height of ten regardless of brightness. Due to the excessive slope, for all edges greater than 20 linear filtering will add too much overshoot and undershoot. This will be true regardless of brightness. The optimum overshoot curves start to flatten for edges greater than 20. This means linear filtering will produce its worst artifacts on the very high contrast edges. This was already known to be true.

It is interesting to plot normalized overshoot height (normalized by the brightness) versus brightness. This is shown in Figure 8. Testing was only done for increasing background brightness. In plotting this curve it was assumed the results would be symmetric about the stripe brightness. The Weber-Fechner law says this fraction should be constant over the entire dynamic range. However, the contrast measurements for each brightness range are sharply convex. The envelope of these convex curves is asymptotically approaching a constant, .02, in a manner predicted by Schreiber for normal viewing

conditions (6). For this experiment, as the difference between the background and the stripe brightness increases, it becomes much more difficult for the eye to perceive artifacts on the edges.

In summary, the subjective testing shows that optimum edge height is an increasing function of edge brightness and contrast. This reaffirms the need for asymmetric shaping. As a function of brightness the overshoot height follows a power law relationship with an exponent of .3 to .5. This is consistent with the power law functions used to minimize the visibility of quantization contours and pseudo-random noise. As a function of contrast, overshoot height increases nonlinearly and the curve starts to flatten for edge heights greater than 20. Because linear filtering adds overshoot proportional to edge magnitude, severe artifacts will be caused on high contrast edges, particularly in the dark tones.

The objective in making these subjective measurements was to determine the appropriate scaling functions for adaptive enhancement. These scaling functions depend heavily on the brightness and contrast measure as well as the optimum overshoot height curves of this chapter. The experimentation to combine these factors into a satisfactory processing function is described in the next chapter.

ADAPTIVE FILTERING EXPERIMENTATION

This chapter explains in detail the experimentation in adaptive filtering. Starting with an initial estimate of the desired scaling functions, these functions were refined through successive cycles of processing and visual evaluations. The initial tuning was done with test pictures containing both low and high contrast edges and a nominal edge radius of 8 pels. In applying these characteristics to real pictures further refinement was needed due to noise and texture considerations. The low pass filter point spread function was reduced to a radius of 4 pels to provide crisper edges. Pictures processed by linear filtering, homomorphic filtering, and Gilkes' adaptive filtering were prepared for comparison. The results indicate that substantially more sharpening is achievable using the experimentally derived scaling characteristics. Results of the application of all four processes to a sample edge are given in Appendix I. No deformation of the edge resulted from the new scaling characteristics. Further experimentation indicated that noise suppression may be another application of adaptive picture processing.

A. PROCESS BLOCK DIAGRAM AND DISCUSSION

A block diagram of the process used for equalized adaptive filtering is shown in Figure 9. The process is equalized in the sense that low, medium, and high contrast edges in both the dark and light tones are sharpened evenly with asymmetric overshoot and undershoot. The original picture, P(X,Y), is

linearly low pass filtered to form L(X,Y) which is subtracted from P(X,Y) to form H(X,Y). H(X,Y) is a high frequency edge version of the original. All edges and detail are still present, but large constant tones are blacked out. This edge picture is scaled, pel by pel, according to local area brightness and contrast before being added to the original picture. The sharpening factor, SF, provides a "sharpening knob" to increase or decrease the overall level of equalized sharpening to suit an observer's particular preference. As SF is turned to zero, only the original picture comes through. Similarly as SF is increased, sharpening increases until artifacts start to appear.

The major components to be optimized are the brightness and contrast scaling functions. The inputs to these functions are the brightness and contrast measures respectively. The brightness measure is the full spectrum original picture pel value. This will cause asymmetric shaping of the edges. The contrast measure is a smoothed gradient. In addition to the scaling functions, an appropriate low pass filter, gradient function, and gradient smoothing process must be determined.

The low pass filtering and gradient smoothing were provided by an existing system convolution program. This program has several limitations. Filter coefficients must be integers between 0 and 255. At the end of processing, the sum of the coefficients is used to normalize the results. This gives a dc gain of one. The program takes the vertical height of

the point spread function and puts that many lines into a buffer. For a picture width of 540 pels, the largest possible point spread function is 9X9 because the buffer size is limited to 4096 bytes. Because normalization is done at the end of the process, the 16 bit accumulator will possibly overflow during intermediate operations if the sum of coefficients exceeds 128.

In view of these limitations, it was decided to use a 9X9 sampled gaussian point spread function for the low pass filtering. This filter is circularly symmetric and thus gives isotropic processing. Because it is separable, the horizontal and vertical filtering can be done sequentially. This is important due to the limitation of 128 on the sum of coefficients. For a separable filter there are only 9 instead of 81 coefficients. A gaussian point spread function convolves with itself to give another gaussian function. This was seen as a way to obtain filters larger than 9X9.

To obtain the filter coefficients, a gaussian function with a standard deviation of 1.375 was sampled. The inter-pel distance was taken as a unit value of one. The coefficients were scaled up by a factor of 120.6 and rounded to the nearest integer. These operations are shown in Figure 10. A standard deviation of 1.375 was chosen so that when the coefficients were scaled up the outermost coefficient would be rounded to one, and the sum of the coefficients would be close to, but not exceed, 128. For the coefficients used the sum was 121. This

gaussian filter resulted in very smooth edge shapes, as can be seen on the linearly filtered test edge of Appendix I.

In this research only two low pass filter point spread functions were used. For a radius of 8 pels, the 9X9 gaussian point spread function was convolved four times with the original picture to give a gaussian function with a standard deviation of 2.75 and a nominal radius of 8. This was used almost exclusively on the test pictures. For the 4 pel radius, the 9X9 function was only convolved once with the original giving a nominal radius of 4. This low pass filtering was used on the photographic images of Section C.

To form a contrast measure, an approximation to the absolute value of the magnitude of the gradient of the original was taken. This function is shown in Figure 11. The averaged absolute value of the horizontal and vertical difference are added together. Although this function is not quite isotropic, no difference could be seen in the treatment of diagonal and horizontal or vertical edges. The original CMAN picture and its gradient are shown in Figures 13 and 14. This measure does a satisfactory job of detecting all edges and detail in the picture. To avoid deforming the edge, the contrast measure must be approximately constant over the entire edge width. The filter used to do this is shown in Figure 12. It is of constant height and roughly circularly symmetric. Because the filtering program divides by the sum of the coefficients, the dc gain is one.

Initially it was thought that an edge radius of 8 would be desirable. To provide a constant contrast measure, the gradient would have to be convolved at least four times and maybe more with the filter of Figure 12. Because of this spreading over a large area, a dc gain of 13 was used in the first 9X9 gradient smoothing to avoid losing low contrast edges. The gradient was then smoothed four more times with a dc gain of one. This contrast measure was used for the test pictures in which the low pass picture was obtained by four gaussian convolutions. No deformation of the edge shape resulted.

When it was decided that an edge radius of 4 pels would give crisper sharpening, the gradient was only smoothed twice by the filter of Figure 12 and both times with a dc gain of one. To avoid losing low contrast edges in this smoothing, before processing, a value of ten was added to the gradient at all pels which were not zero. This contrast measure was found to be very satisfactory for an edge radius of 4 pels. No edge shape deformation occurred. A sample edge processed by both the 8 wide gaussian point spread function with the five times convolved gradient contrast measure and the 4 wide gaussian point spread function with the twice convolved gradient contrast measure is shown in Appendix I.

B. TEST PICTURE EXPERIMENTATION

To adjust the brightness and contrast scaling characteristics, test pictures with both low and high contrast edges were made. The pictures consisted of four 80X80 pel blocks on a constant background. Two of these pictures were used for adjustment. Picture TEST1 has a background brightness of 20 and block brightnesses of 30, 40, 60 and 120. TEST1 is shown in Figure 15. Picture TEST2 has a background brightness of 100 and block brightnesses of 110, 120, 140, and 200. It was felt that these pictures sufficiently covered the tone scale and contrasts of interest.

The initial estimate for the brightness scaling function followed the overshoot versus brightness curve of Chapter II, with brightness plotted in internal values of 0 to 255. The only changes made were in the extreme low and high brightness regions. If edges at the end of the brightness scale are sharpened, they will possibly exceed the dynamic range. To avoid compression of the dynamic range, the sharpening was reduced to zero at both ends of the scale. Only slight modification was made to this curve during test picture adjustment. The adjusted brightness characteristic is shown in Figure 16.

The low passed test picture was obtained from the original by convolving the original four times with the gaussian point spread function. This gave an edge width of about 8 pels. It was quickly discovered in the test picture experimentation that if edge shape distortion was to be avoided, the gradient picture

had to be convolved with the constant height 9X9 filter of Figure 12 five times, one more than in forming the low pass picture. A dc gain of 13 was used to avoid losing the low contrast edges in this extensive smoothing.

No fixed relationship existed between the smoothed gradient contrast measure and the contrast measure (edge magnitude) used in Chapter II. The overshoot versus contrast results of Chapter II show that linear filtering adds excessive overshoot to edges greater than 20. The contrast scaling function should certainly be a decreasing function in this range. To avoid amplifying noise, the sharpening of very low contrasts should also be small. This leaves the majority of sharpening in the middle contrasts. An initial estimate with this type of characteristic was formed and then refined through visual evaluation. The resultant characteristic which appeared to successfully balance the sharpening between low and high contrast edges is shown in Figure 17.

In both brightness and contrast scaling functions, it's the relative magnitude between dark and light tones and low and high contrasts that is important. The absolute magnitude of the scaling is adjusted by varying the SF value. In adjusting the scaling curves, sharpening was increased using SF until artifacts started to appear. Refinement of the characteristics to balance artifacts was done and the processing then repeated.

An example of equalized adaptive filtering on TEST1 is given in Figure 18. Comparison pictures done with linear,

Gilkes, and homomorphic filtering are shown in Figures 19-21. The low pass filtering for these comparison pictures was also done using the four times convolved gaussian point spread function. From these pictures it is easy to see the balanced sharpening of the equalized adaptive filtering. The linearly filtered and Gilkes filtered edges have very bad dark band artifacts on the high contrast edge. Homomorphic filtering leaves a light band artifact on the high contrast edge. The equalized adaptive filtering is the only process which brings up the sharpening evenly. At this point it was appropriate to test the process on photographic images.

C. ENHANCEMENT OF PHOTOGRAPHIC IMAGES

The test pictures had no texture areas and no noise because they were computer generated. When the scaling characteristics of Figures 16 and 17 were applied to actual photographic pictures several problems were encountered. In the gradient picture texture and noise both result in areas of approximately constant gradient. This is fundamentally different from the gradient of edges which are localized to the contours of objects. The noise had a very low gradient value. The texture areas had both medium and high gradient values.

The dc gain of 13 used in the gradient smoothing was intended to aid edges from being eliminated when they were spread over a large area. This was successful for the edges but was unsuitable for the texture and noise. Low gradient areas of

noise were amplified by a factor of 13 into the middle, "high sharpness" part of the contrast characteristic. Texture areas were amplified into the very high contrast part of the curve and, as a result, were hardly sharpened at all.

Another unsatisfactory effect was the sharpening of the contours of very large objects. The use of an 8 pel edge radius left macro area contours looking dull. It was decided to reduce the radius to 4 pels to try to produce crisper eges. This gave a more satisfactory result.

To obtain a four wide edge only a single convolution of the gaussian point spread function with the original picture is needed. Brief experimentation with the test pictures showed that edge deformation could be avoided if the gradient picture was convolved twice with the constant height filter of Figure 12. To avoid the problem with noise and texture, a dc gain of one was used. To keep from losing low contrast edges, before smoothing, a value of ten was added to the gradient everywhere it wasn't zero. This had a small effect on the noise and texture, but nowhere near the severe change of the earlier multiplication. The smoothed gradient CMAN picture is shown in Figure 22.

Without the multiplication factor of 13, the contrast measure was lower and the contrast scaling function had to be readjusted. The adjustment was made by processing four photographic images repeatedly and evaluating the results. In this adjustment, the brightness scaling characteristic was reduced

slightly in the high brightness range to reduce light band overshoot. The final adjusted characteristics are shown in Figure 23 and 24. The four processed pictures are shown in Figures 25, 30, 35, and 40.

Comparison pictures done with linear, Gilkes, and homomorphic filtering are also shown. The low pass filter used in their processing was a one-time convolution with the gaussian point spread function. The details of these processes are given in Appendix I. The sharpening in the linear and Gilkes pictures was scaled such that artifacts were just starting to occur. In this way their ability to sharpen without artifacts can be compared to the equalized adaptively filtered pictures.

The homomorphic pictures were done with a dc gain of .875 rather than the .5 value Stockham used (15). The CMAN picture, homomorphically filtered with a dc gain of .5, is shown in Figure 44. The tone scale is grossly compressed. Examination of Stockham's reported pictures shows no similar severe compression to the very dark tones. Evidently this must be due to a difference in the internal computer representation. The dc gain of .875 produces tone changes similar to the pictures reported.

For both the CMAN and the BANK pictures, equalized adaptive filtering clearly produces the sharpest pictures before artifacts occur. Because these pictures have high contrast edges, linear and Gilkes sharpening must be turned down to

avoid artifacts. As a result, low and medium contrast edges and detail in those pictures are not sharpened enough. The homomorphic filtering produces artifacts on the high contrast edges and does a very poor job of enhancing low contrast detail and edges. In fact, in the homomorphic CMAN picture, visibility of one of the background buildings is actually less than in the original.

The original pictures are derived from the photographic image by laser scanning and then outputting to the Laserphoto Receiver. The equalized adaptive filtering was so effective in bringing up low contrast detail that even in comparison with the source pictures, enhancement of detail could be seen. Of course, the overall quality of the enhanced pictures was not as good as the source image.

There were no high contrast edges in the OLEH and DOC pictures. As a result, linear, Gilkes, and homomorphic filtering were more successful than in CMAN and BANK. More enhancement of low contrast detail was possible because sharpening could be turned up more. Equalized adaptive filtering was more effective than the others in sharpening the low gradient texture on the faces. Due to the nature of the pictures, this sharpening limited the overall enhancement of the equalized adaptively filtered pictures. Human observers are very sensitive to facial texture. Texture sharpening that is acceptable on the walls of the BANK becomes unnatural on a face. This fact indicates that possibly no single set of characteristics

will be optimum for all pictures. A certain set may be better for some class of pictures. A general purpose set of scaling characteristics would have to compromise between the various picture classes.

The only unsatisfactory aspect of equalized adaptive filtering is its sharpening of high gradient texture. The contrast measure makes it impossible to distinguish this texture from high contrast edges. To avoid artifacts, the high contrast edges must be scaled down. Unfortunately, this also causes a reduction in the sharpening of the high gradient texture. That sharpening is desirable. Examples where this texture could have been sharpened more are OLEH's coat and moustache. No satisfactory solution to this high gradient texture sharpening was found.

D. NOISE SUPPRESSION EXPERIMENTS

A potential application of adaptive filtering is noise suppression. A noisy picture may be blurred to reduce the noise. The blurred picture can then be adaptively sharpened to restore the edges to their initial state or to further enhance the picture.

An experiment was done to reduce the noise in Figure 45. This is a four bit per pel version of the original eight bit per pel CMAN picture. Pseudo-random noise was added before quantization to four bits, then subtracted (21). No nonlinear transformation was used in the quantization process. To

suppress the noise this picture was blurred by the 3X3 filter:

$$\begin{matrix} 1 & 1 & 1 \\ 1 & 1 & 1 \\ 1 & 1 & 1 \end{matrix}$$

The convolution program divides by the sum of coefficients to give a dc gain of one.

The blurred picture was then adaptively enhanced using the gaussian point spread function with a radius of 4 pels. The resulting picture is shown in Figure 46. The noise in the dark constant parts of the picture is significantly reduced. The background buildings are sharpened and more visible than in the original 8 bit CMAN picture.

The sharpening was limited by the start of artifacts on high contrast edges. As a result, edges of macro areas are slightly less sharp than originally. The easy visibility of the light band artifacts is probably due to the widening of the edge beyond 4 pels by the initial 3X3 smoothing.

CONCLUSIONS

This work was undertaken to determine if subjectively better pictures could be produced by equalizing the sharpening of low and high contrast edges in an adaptive filtering scheme. The results indicate that significantly more sharpening can be achieved before artifacts start to occur.

The experimentally derived brightness and contrast scaling characteristics are very effective on the CMAN and BANK photographs. Due to the sensitivity of human observers to facial texture, these characteristics are less successful on DOC and OLEH. This leads to the conclusion that probably no one set of characteristics will be satisfactory for all pictures. A certain class of pictures that have similar edge and texture requirements could be served by a single set of functions. Other classes would require another set. For example, a contrast scaling function that suppresses low gradient texture would be more appropriate for portrait photographs with no high contrast edges. If one set of scaling functions was to be used for general purpose enhancement, it would have to compromise among the different picture classes.

To avoid the deformation of edge shape encountered in Gilkes' adaptive filtering, a smoothed gradient contrast measure was used. The gradient measure had to be smoothed so that it was wider than the edge width. This was very successful in avoiding edge deformation, but the use of a gradient contrast measure did result in one disadvantage. High gradient texture

could not be distinguished from high contrast edges and thus the sharpening was reduced. No satisfactory method of increasing this texture's sharpness was found. This would be an interesting area for future research.

The original, full spectrum, pel value was used as a brightness measure. This caused the proper asymmetric edge shaping that was not achievable with a low passed brightness measure. Tone scale compression was avoided by reducing the brightness scaling function to zero at both ends of the dynamic range. No artifacts due to saturation on either end of the tone scale were visible in any picture.

An edge width of four pels was desirable for the pictures used in this research. For other pictures, wider edge widths may be appropriate. This will require greater smoothing of the gradient which means certain edge heights will map into different contrast measures. The contrast scaling characteristics must be adjusted to allow for this. More work is needed to calibrate the relation between increased gradient smoothing and shift of the contrast scaling function.

Another application of adaptive filtering is noise suppression. Noisy pictures may be smoothed, blurring the noise, then adaptively filtered to recover the edges. Edges of large objects suffer slightly from this process. Small objects and detail can be recovered and enhanced beyond their original quality.

As part of the investigation of adaptive filtering, subjective testing was done to determine optimum overshoot height as a function of brightness and contrast. The results show that optimum overshoot height is an increasing function of both contrast and brightness. As a function of brightness, the overshoot follows a power law form. This implies the eye's nonlinear perception of brightness is close to a power law. As a function of contrast, the overshoot height increases nonlinearly and flattens out for edges greater than 20. It can be seen that for edges greater than 20, linear sharpening adds excessive overshoot and undershoot. The results are consistent with previous knowledge of the nonlinearity of human vision. Further experimentation to determine the relationship between optimum overshoot height and edge width is a possible area for future investigation.

APPENDIX I

Four forms of processing were applied to the one dimensional, high contrast edge of Figure 47. The darker tone is 100 and the lighter tone 200 on the PDP 11/40 internal scale of 0 to 255. The output pictures were inspected on a pel by pel basis to obtain these results.

For all four processes the low pass filtering block consists of four sequential convolutions using the 9X9 gaussian point spread function of Figure 10. Because this point spread function is separable, each convolution involves a horizontal and vertical pass. The nine coefficients used are explained in Chapter III. This low pass filter was used for linear, homomorphic, Gilkes adaptive and equalized adaptive processing of the one dimensional edge. A single convolution was used to obtain the low pass filtered picture of the 4 pel edge radius equalized adaptive filtering.

A. LINEAR FILTERING

A block diagram of the linear filtering and the resulting edge is shown in Figure 48. Subtracting the low pass version from the original leaves the high frequency edge picture. By adding these high frequency components back to the original, a high pass filtered picture is formed. Symmetric overshoot and undershoot are added to the edge. The expected overshoot height of 50 was reduced to 44 by round off error in the

filtering process. The multiplication by SF allows scaling of the edge signal. This scaling was used in Chapter III to produce linearly filtered pictures without artifacts. For this one dimensional edge, the value SF=1 was used.

B. HOMOMORPHIC FILTERING

A block diagram of the homomorphic filtering process and the resulting edge is shown in Figure 49. The logarithm used is a scaled and shifted version of a base 10 logarithm:

$$255(\mathrm{LOG}(B+1))/\mathrm{LOG}(256) \qquad 0 \leqslant B \leqslant 255$$

This was necessary to keep the logarithm picture within the allowed 0 to 255 range of the computer system. Homomorphic filtering changes the brightness of the edge and reduces the contrast. It does produce asymmetric shaping of the edge. However, it adds excessive overshoot to the high contrast edges. The overshoot height of 50 is larger than that added to the linearly filtered edge. Because this overshoot is added to the lower brightness level of 112 rather than 200 it is obviously excessive.

The low passed logarithm picture is scaled by .5625 to provide a dc gain of .875. The reduction of macro area contrast, seen as the shifting of the one dimensional edge from 100-200 to 62-116, is caused by a dc gain of less than one.

C. GILKES ADAPTIVE FILTERING

A block diagram of Gilkes adaptive filtering scheme and its affect on the one dimensional edge is shown in Figure 50. The scaling function on the edge signal is also given. The brightness measure is the low passed picture pel value. The contrast measure is the pel value of the edge signal. The multiplication by SF allows further scaling of the already scaled edge picture. This ability was used in Chapter III. For this one dimensional edge, the value SF=1 was used.

Approximately symmetric overshoot is added to the edge as a result of using the slow varying low pass filtered picture as a brightness measure. The shape of the edge is severely distorted because the contrast measure is the sharply varying edge signal. Both overshoot and undershoot height are much less than the linearly filtered edge. However, the edge distortion still results in some visible artifacts.

D. EQUALIZED ADAPTIVE FILTERING

The block diagram for equalized adaptive filtering is given in Chapter III. The results of this processing using the 8 pel radius low pass filter is shown in Figure 51. The low pass filter used for this result was the four times convolved gaussian point spread function. A value SF=7 was used. This turned up the sharpening as high as possible without artifacts. The scaling functions of Figures 16 and 17 were used.

The edges are asymmetrically shaped and their shape is not distorted. The overshoot and undershoot is much less than the linearly filtered edge. Although the overshoot height is greater than that added by Gilkes processing, no artifact is seen because the edge is not distorted.

For comparison, the one dimensional edge is adaptively filtered using a 4 pel radius point spread function. The result is shown in Figure 52. The low pass filter is the once convolved gaussian function. A value SF=6 was used. The scaling functions of Figures 23 and 24 were used. The overshoot and undershoot heights are slightly greater but this is to be expected due to the smaller edge width. As before, the edge is not distorted.

APPENDIX II

The traditional view of the eye's static nonlinear perception of brightness is:

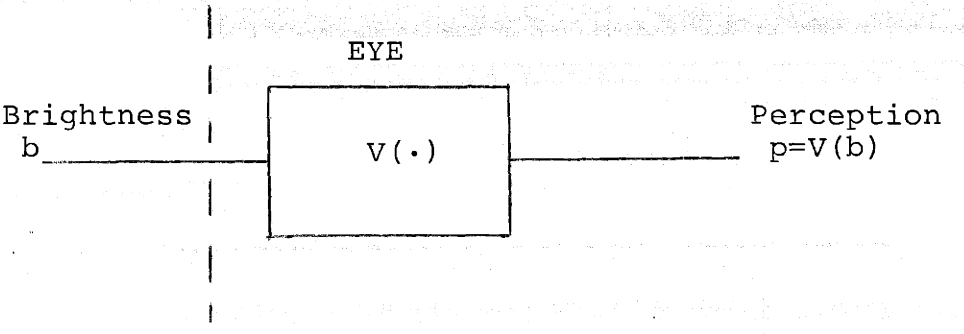

Weber's experiments indicated that the $\Delta b \int b$ causing a just noticeable difference was approximately constant over a wide range of brightness levels. The usual assumption is that the Δp change in perception is constant for all brightness levels. The ratio $\Delta p \int \Delta b$ approximates the derivative of the p versus b curve because these measurements are for very small, threshold changes.

$$\Delta p = K1$$

$$\Delta b = K2 \cdot b$$

$$dp/db = \Delta p/\Delta b = K3/b$$

$$p = K3 \cdot LOG(b) + C$$

K1, K2, K3, and C are constants. This is the basis for modelling the eye as a logarithmic detector.

In minimizing the visibility of Roberts pseudo-random noise, it was found that a better model for the eye's nonlinear perception is of the form: (11), (12):

$$p = K \cdot LOG(1+ab)$$

with a value of a=.125 and K is a constant. For a dynamic range of 1.6 log units or a brightness ratio of 40:1, the normalized relation is (17):

$$p = 39 \frac{\text{LOG } (1+ab) - \text{LOG } (1+a)}{\text{LOG } (1+40a) - \text{LOG } (1+a)} + 1$$

$$\frac{\Delta p}{\Delta b} = \frac{K4}{\Delta b} = \frac{dp}{db} = \frac{K5}{1+ab}$$

$$\Rightarrow \quad \Delta b = K6 \ (1+ab) = K6 \ (1+.125b)$$

$$1 \leq b \leq 40$$

where K4, K5, and K6 are constants.

A power function has also been used to minimize the visibility of quantization contours and pseudo-random noise (12). For the dynamic range here it's of the form (17):

$$p = 39 \frac{b^{.5} - 1}{40^{.5} - 1} + 1$$

$$\frac{\Delta p}{\Delta b} = \frac{K7}{\Delta b} = \frac{dp}{db} = K8 \cdot b^{.5}$$

$$\Delta b = K9 \cdot b^{.5}$$

$$1 \leq b \leq 40$$

where K7, K8, and K9 are constants.

The assumption that Δp is constant, independent of brightness is unrealistic (summarized in 8). Communication theory indicates that the significant parameter in detection is the signal to noise ratio. In many cases, the signal noise increases as the level of the signal increases. Photon noise associated with the input stimulation increases as the square root

of the brightness, and photographic noise increases with the density level. It seems very likely that a greater Δp is required for detection at higher levels of brightness.

APPENDIX III

The overshoot shapes used in the subjective testing experiments of Chapter II are tabulated in Figure 53. The same shapes were used for overshoot and undershoot. When an overshoot height was specified, the tabulated edge shape was added to the ten closest pels on the brighter side of the edge. When an undershoot height was specified, the tabulated edge shape was subtracted from the ten closest pels on the darker side of the edge.

The subjective testing results for all eight subjects are given in Figures 54 and 55. The average value is obtained by dropping the high and low response and averaging the remaining six. The overshoot versus contrast results are then further smoothed within each brightness group. Each average is added to the one above and below it, then divided by three. The endpoints of 5 and 30 are added to themselves and the next interior value, then divided by three. The overshoot versus brightness results are taken as a single group and smoothed four times by the same smoothing process. Intermediate smoothed values are tabulated in Figure 55.

FIGURES

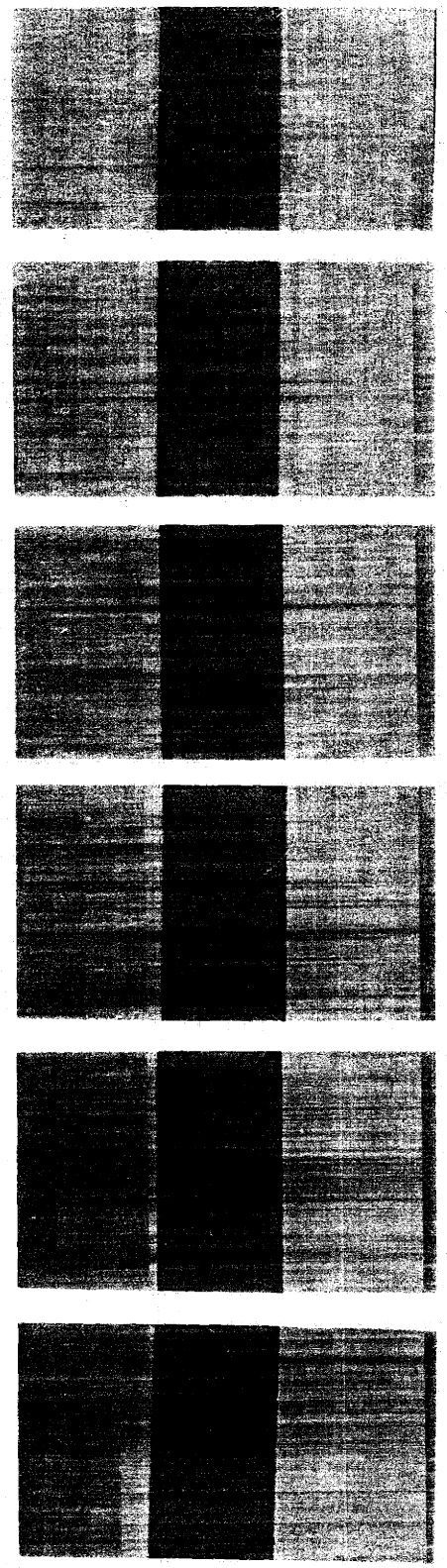

Figure 1. Subjective Testing Example Page

BRIGHTNESS Stripe	Backgr.	OVERSHOOT,UNDERSHOOT #1	#2	#3	#4	#5	#6	#7
20	25	0,0	2,2	3,2	3,3	4,3	5,4	x
40	45	0,0	2,2	4,3	5,4	6,6	x	x
60	65	0,0	2,2	4,4	6,6	8,8	10,10	x
80	85	0,0	2,2	4,4	6,6	8,8	10,10	x
100	105	0,0	3,3	5,5	7,7	9,9	11,11	x
120	125	0,0	5,5	7,7	9,9	11,11	13,13	15,15
145	150	0,0	8,7	10,10	13,13	16,16	x	x
170	175	0,0	8,7	11,10	14,13	17,16	20,19	x
210*	215	0,0	2,2	4,4	5,5	6,6	7,7	8,8

* Prepared after a change in photographic paper

Figure 2. Overshoot versus Brightness Test Page Listings

BRIGHTNESS		OVERSHOOT,UNDERSHOOT						
Stripe	Backgr.	#1	#2	#3	#4	#5	#6	#7
60	65	0,0	2,2	4,4	6,6	8,8	10,10	x
60	70	0,0	2,2	5,5	8,8	11,11	x	x
60	75	0,0	4,3	7,6	10,9	13,12	x	x
60	80	0,0	6,5	9,8	12,11	15,14	x	x
60	90	0,0	7,5	10,8	13,11	16,14	x	x
100*	105	0,0	3,3	5,5	7,7	9,9	11,11	x
90	100	0,0	3,3	5,5	8,8	10,10	12,12	x
90	105	0,0	4,3	6,5	9,8	11,10	15,14	x
90	110	0,0	5,4	7,6	9,8	11,10	13,12	15,14
90	120	0,0	6,5	8,7	10,9	12,11	14,13	16,15
145	150	0,0	8,7	10,10	13,13	16,16	x	x
145	155	0,0	8,7	10,10	13,13	16,16	x	x
145	160	0,0	11,10	14,13	17,16	20,19	x	x
145	165	0,0	11,10	14,13	17,16	20,19	x	x
145	175	0,0	12,10	15,12	18,16	21,19	x	x
170**	175	0,0	8,7	11,10	14,13	17,16	20,19	x
175***	185	0,0	4,4	6,6	8,8	10,10	12,12	14,14
175***	190	0,0	6,5	8,7	10,9	12,11	14,13	16,15
175***	195	0,0	7,6	9,8	11,10	13,12	15,14	17,16
175***	205	0,0	6,5	8,7	10,9	12,11	14,13	16,15

* Same Reflection Density as 90
** Same Reflection Density as 175
*** Prepared after a change in photographic paper

Figure 3. Overshoot versus Contrast Test Page Listings

BRIGHTNESS Stripe	Backgr.	SMOOTHED OVERSHOOT (SO)	SO/Backgr.
60	65	3.72	.0572
60	70	4.00	.0571
60	75	5.22	.0696
60	80	8.06	.1008
60	90	10.00	.1111
100	105	5.17	.0492
90	100	5.61	.0561
90	105	6.55	.0624
90	110	7.61	.0692
90	120	8.89	.0741
145	150	5.78	.0385
145	155	6.69	.0432
145	160	7.61	.0476
145	165	9.93	.0602
145	175	11.12	.0635
170	175	4.61	.0236
175	185	6.03	.0326
175	190	7.72	.0406
175	195	8.83	.0453
175	205	9.38	.0458

Figure 4. Overshoot versus Contrast Results

BRIGHTNESS Stripe	BRIGHTNESS Backgr.	SMOOTHED OVERSHOOT	REFLECTION DENSITY (D)	$10^{1.6-D}$
20	25	3.61	0.50	3.2
40	45	3.69	0.80	6.3
60	65	3.87	1.05	11.2
80	85	4.14	1.10	12.6
100	105	4.54	1.30	20.0
120	125	4.94	1.35	22.4
145	150	5.23	1.40	25.1
175	180	5.32	1.50	31.6
210	215	5.31	1.55	35.5

Figure 5. Overshoot versus Brightness Results

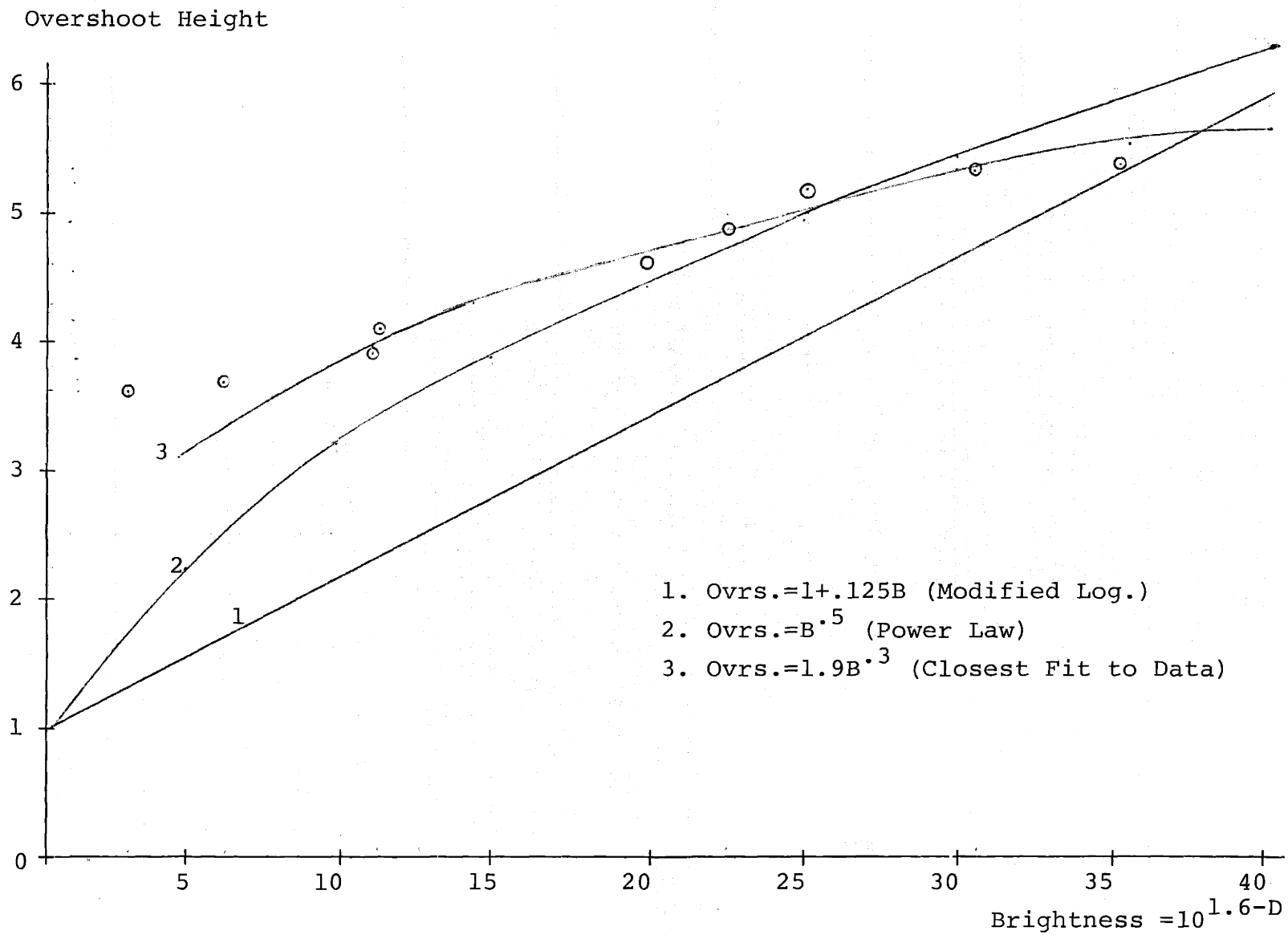

Figure 6. Overshoot versus Brightness Plot

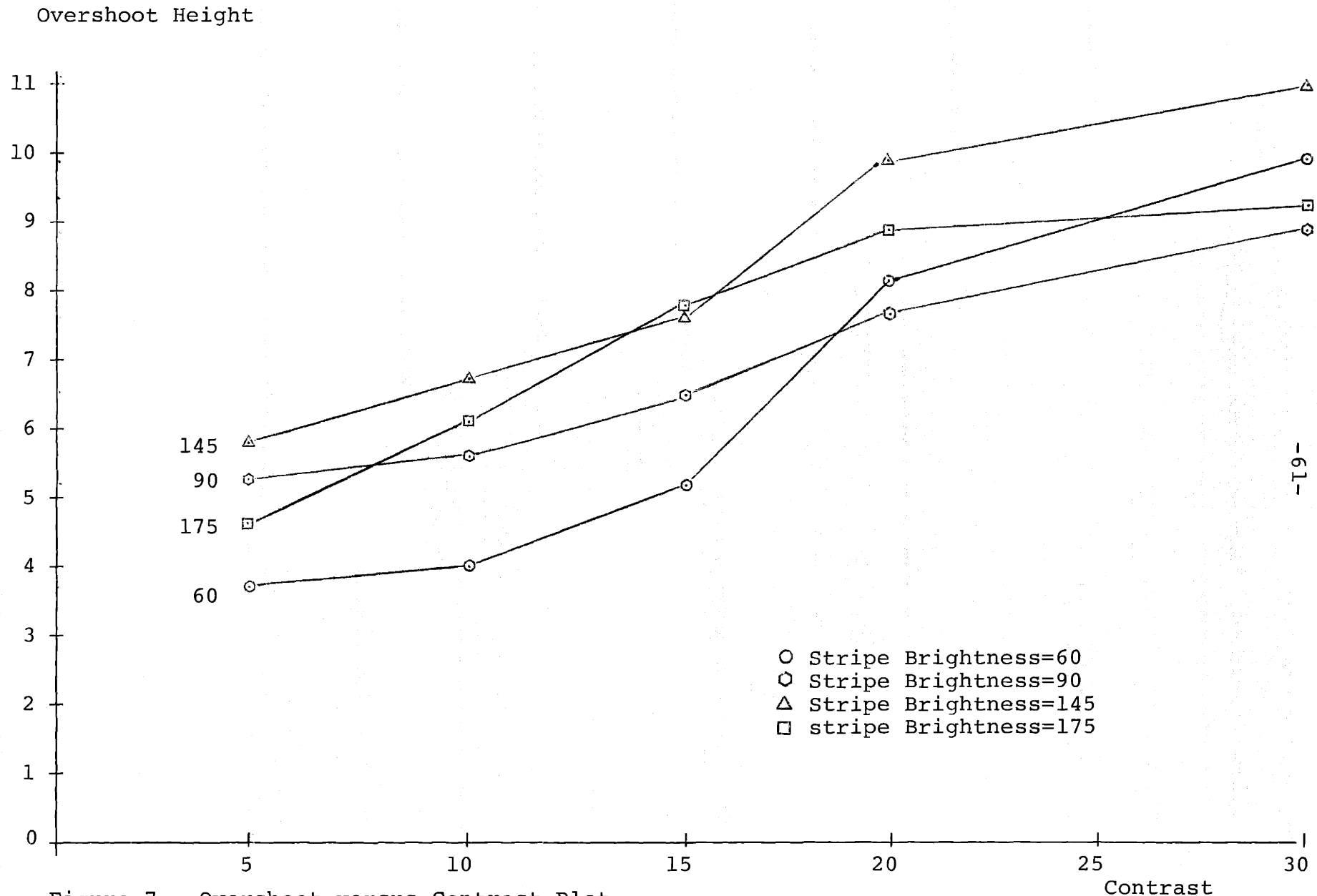

Figure 7. Overshoot versus Contrast Plot

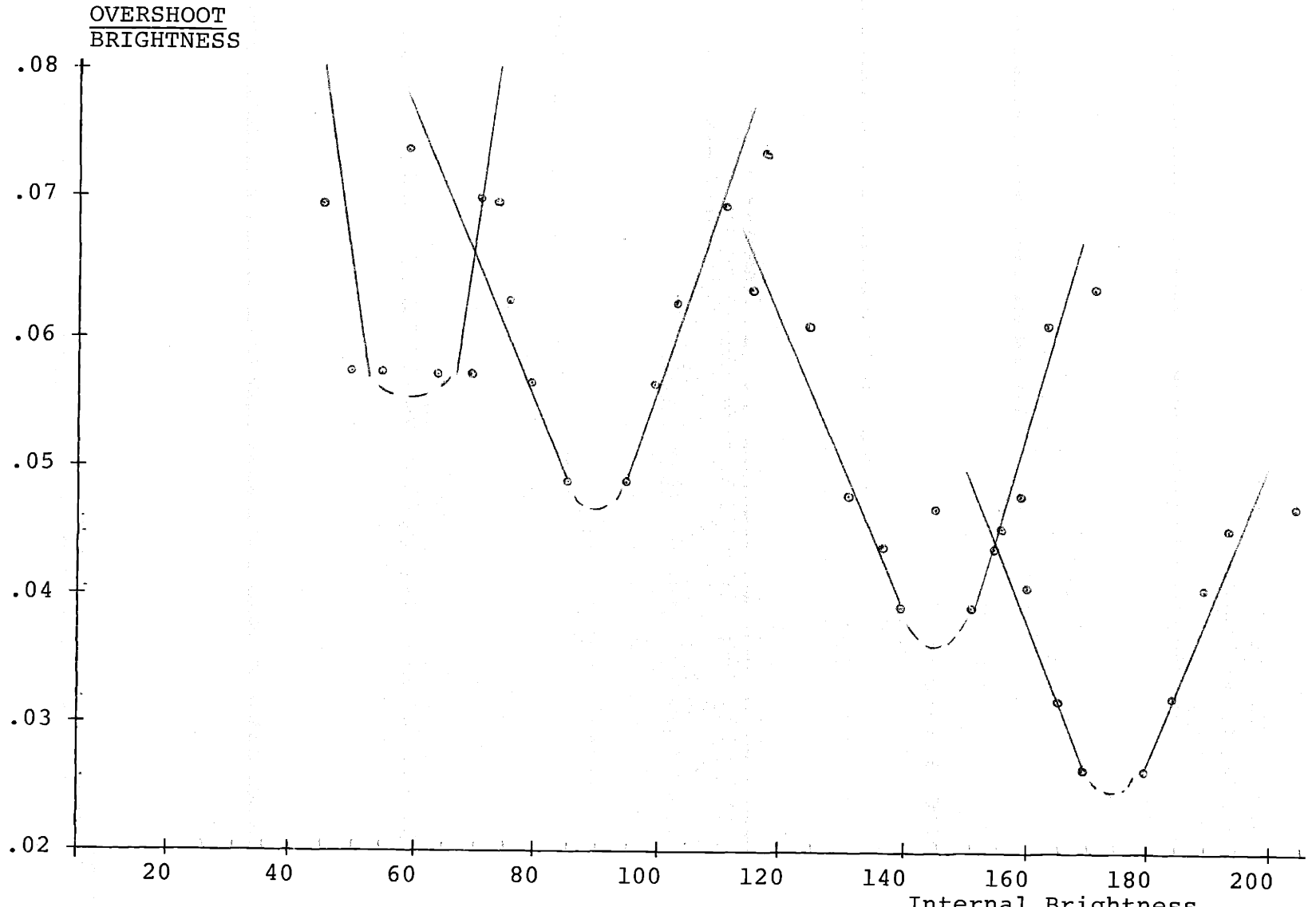

Figure 8. Contrast Results: $\frac{\text{Overshoot}}{\text{Brightness}}$ versus Brightness (Internal)

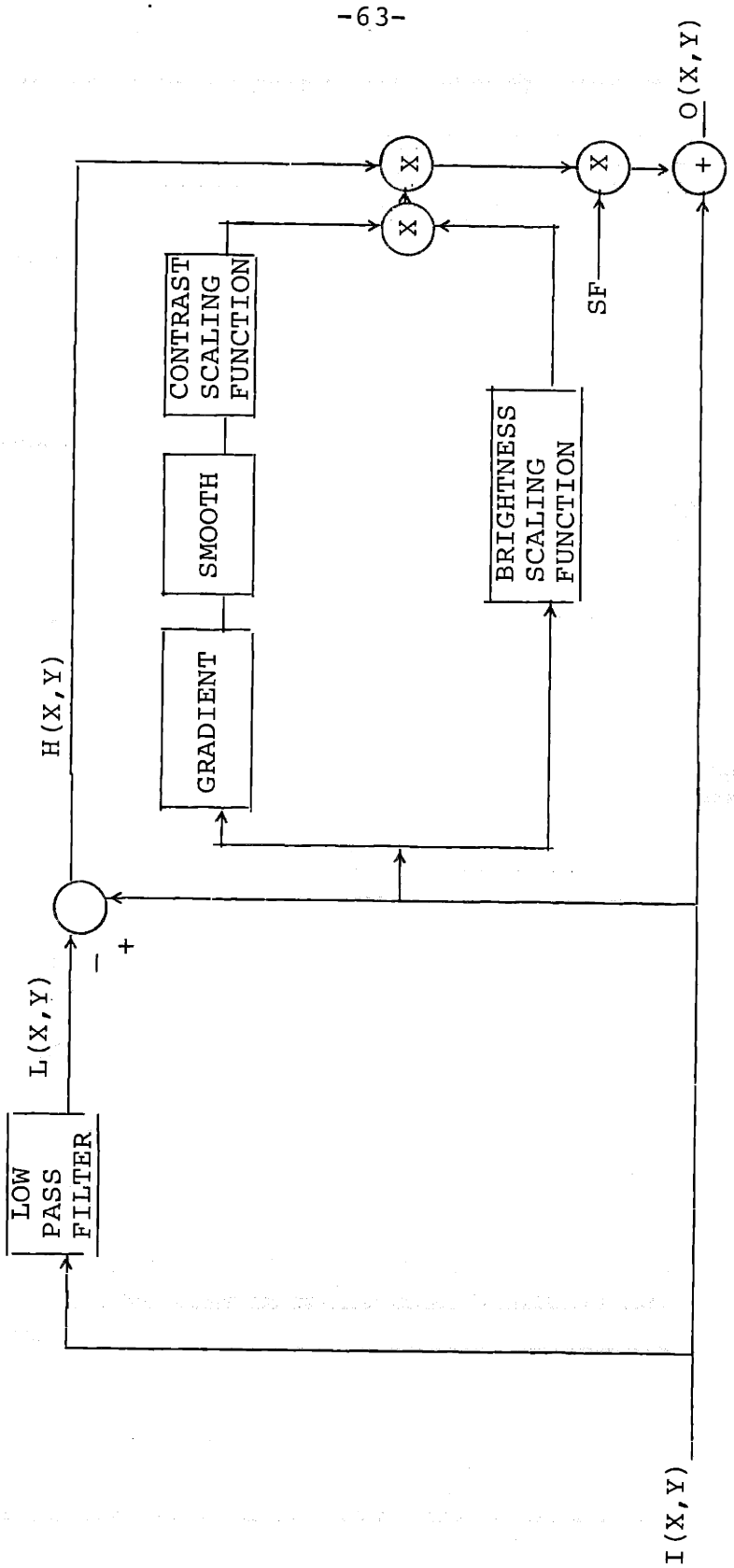

Figure 9. Block Diagram for Equalized Adaptive Filtering

$$g(x) = (2\pi v)^{.5} \exp(-x^2/2v)$$

$$v = (1.375)^2$$

x	g(x)	(120.6)·g(x)	Rounded to Nearest Intger
0	.29014	34.991	35
1	.22272	26.860	27
2	.10074	12.149	12
3	.02685	3.238	3
4	.00422	0.509	1

1X9 Sampled Point Spread Function

1 3 12 27 35 27 12 3 1

Figure 10. Sampled Gaussian Point Spread Function

$$\begin{array}{ccc} & D & \\ B & A & C \\ & E & \end{array}$$

$$\text{Gradient} = \frac{|A-B|}{2} + \frac{|A-C|}{2} + \frac{|A-D|}{2} + \frac{|A-E|}{2}$$

Figure 11. Approximation to Absolute Value of the Magnitude of the Gradient

0	0	0	1	1	1	0	0	0
0	0	1	1	1	1	1	0	0
0	1	1	1	1	1	1	1	0
1	1	1	1	1	1	1	1	1
1	1	1	1	1	1	1	1	1
1	1	1	1	1	1	1	1	1
0	1	1	1	1	1	1	1	0
0	0	1	1	1	1	1	0	0
0	0	0	1	1	1	0	0	0

Figure 12. Filter Coefficients for Gradient Smoothing, 9X9

Figure 13. CMAN, Original

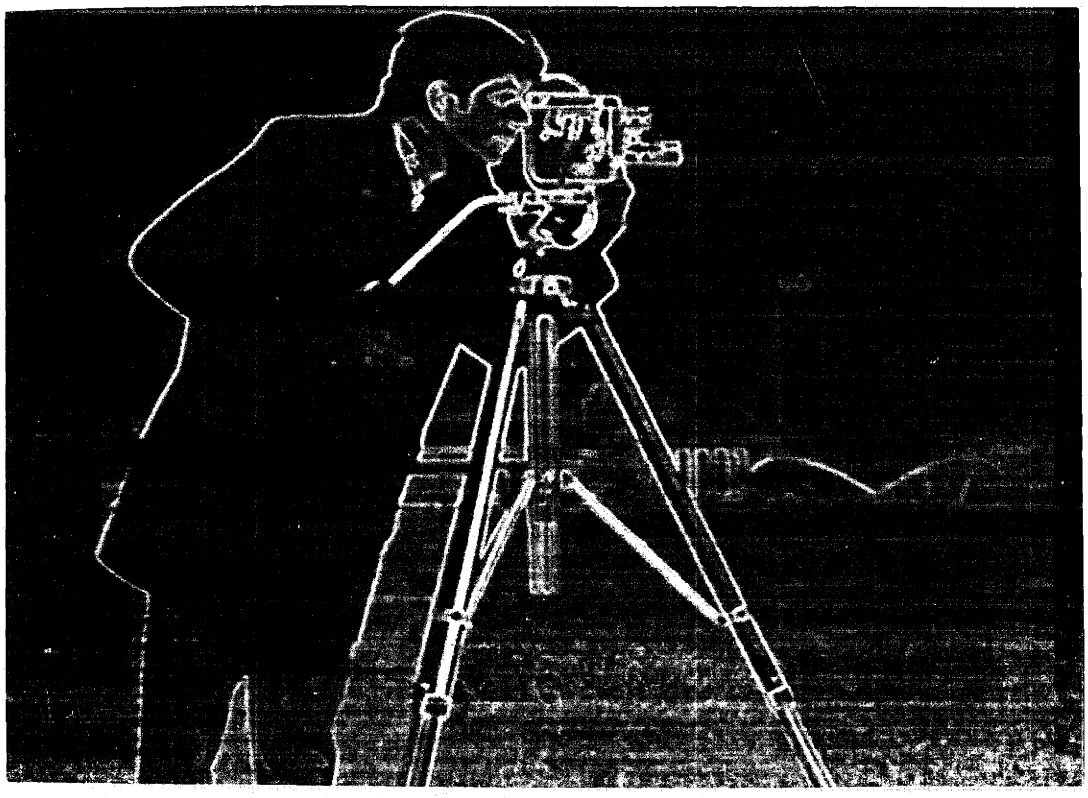

Figure 14. CMAN, Gradient Picture

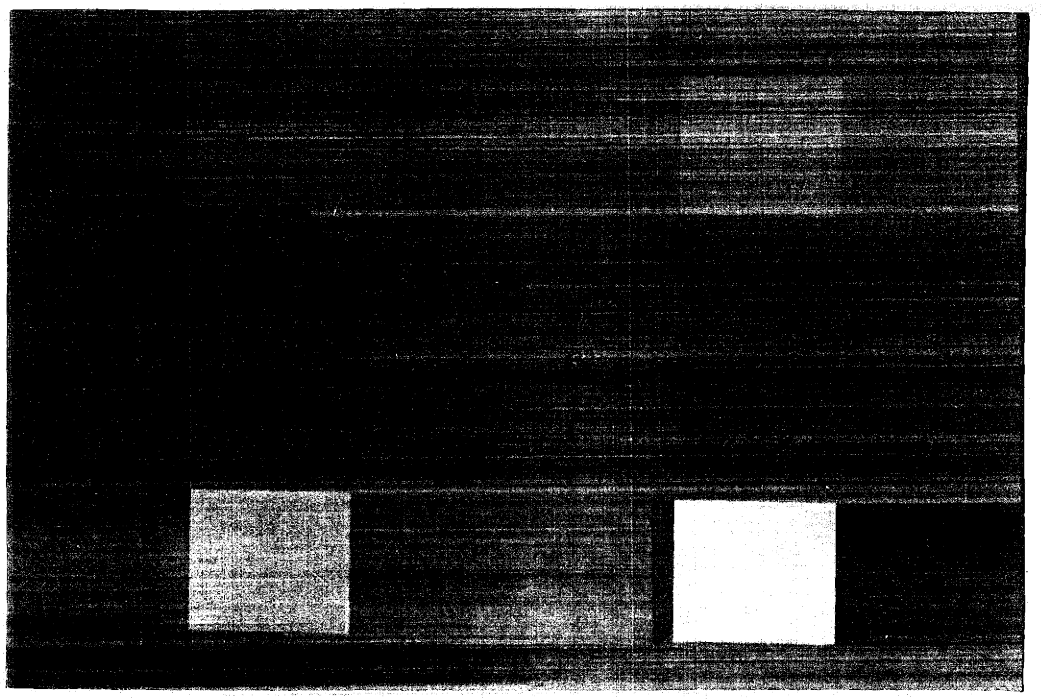

Figure 15. TEST1, Original

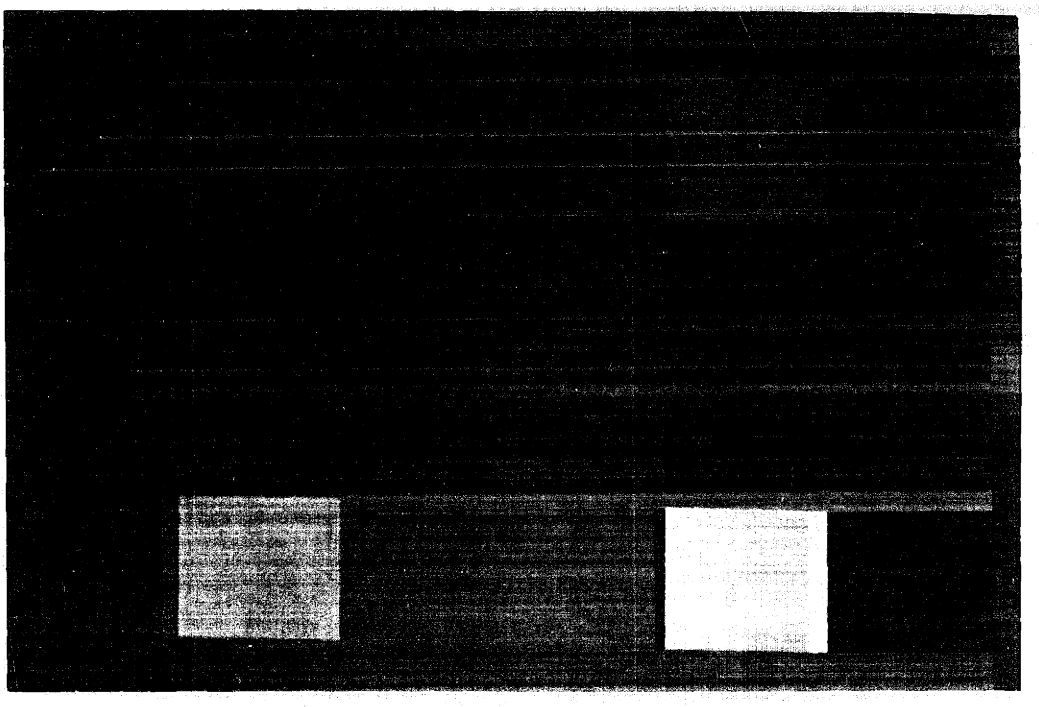

Figure 18. TEST1, Equalized Adaptive Filtering, SF=7

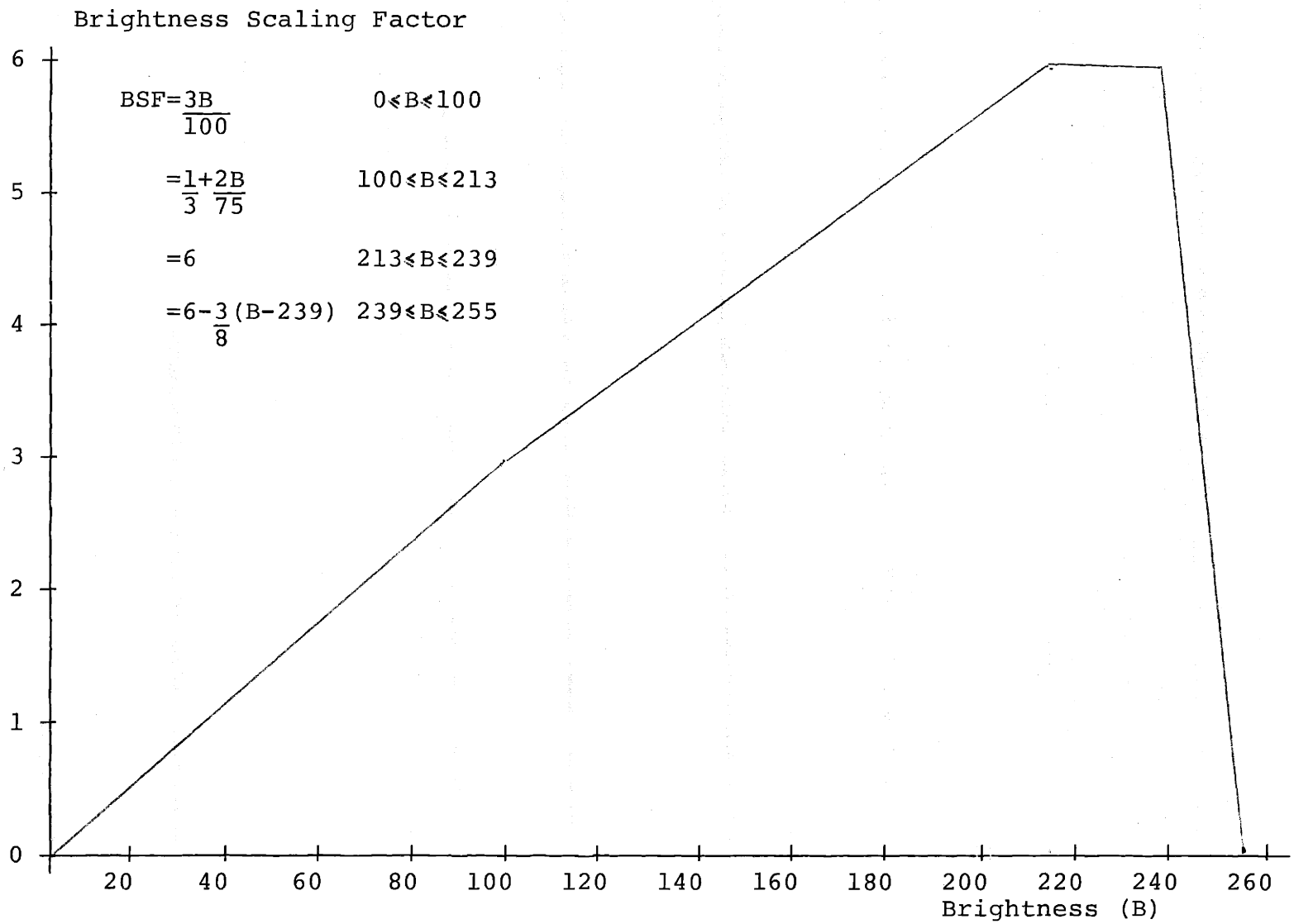

Figure 16. Brightness Scaling Function, 8 pel edge radius

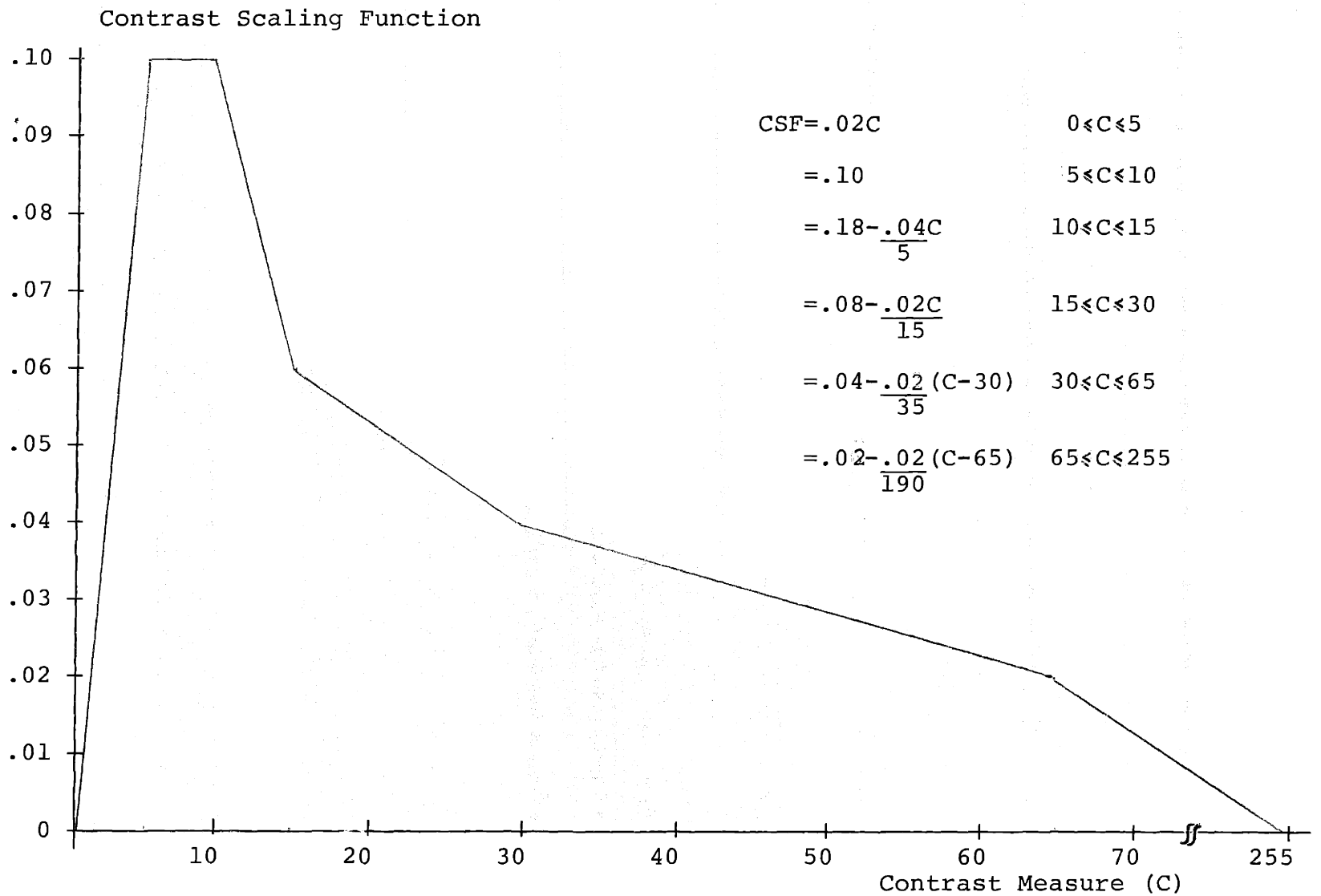

Figure 17. Contrast Scaling Function, 8 pel edge radius

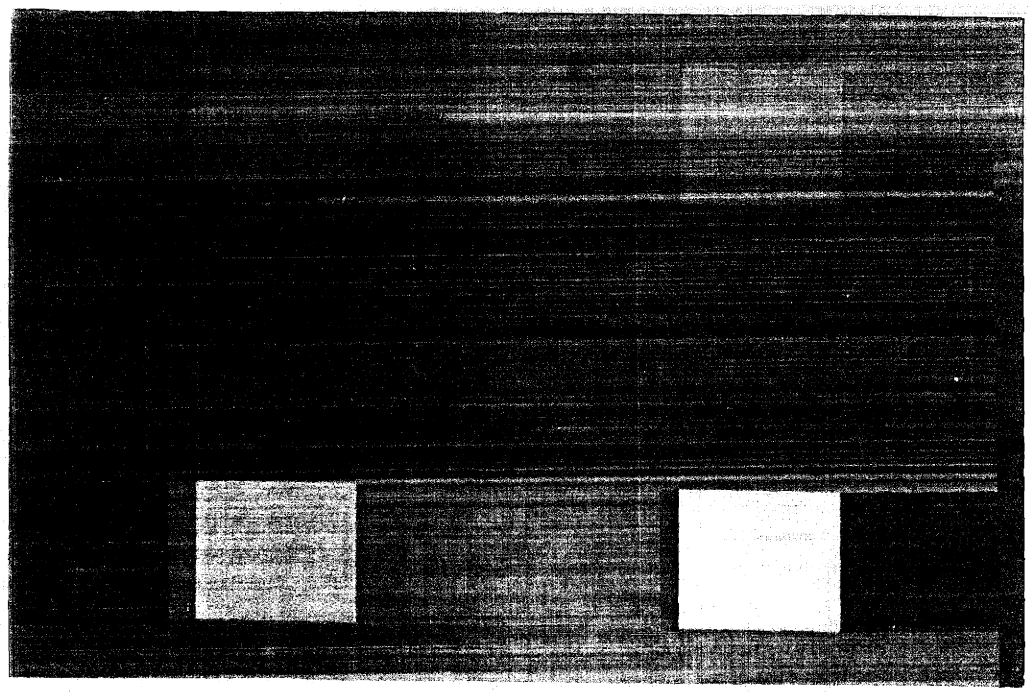

Figure 19. TEST1, Gilkes Adaptive Filtering, SF=1

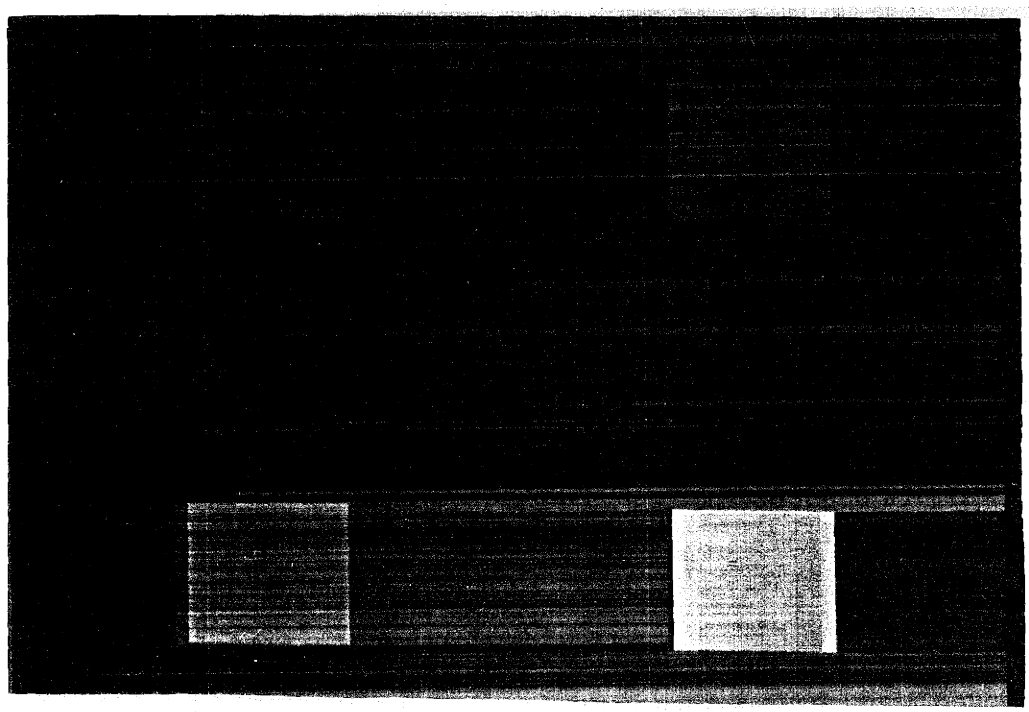

Figure 20. TEST1, Homomorphic Filtering, dc gain=.875, ∞ gain=2

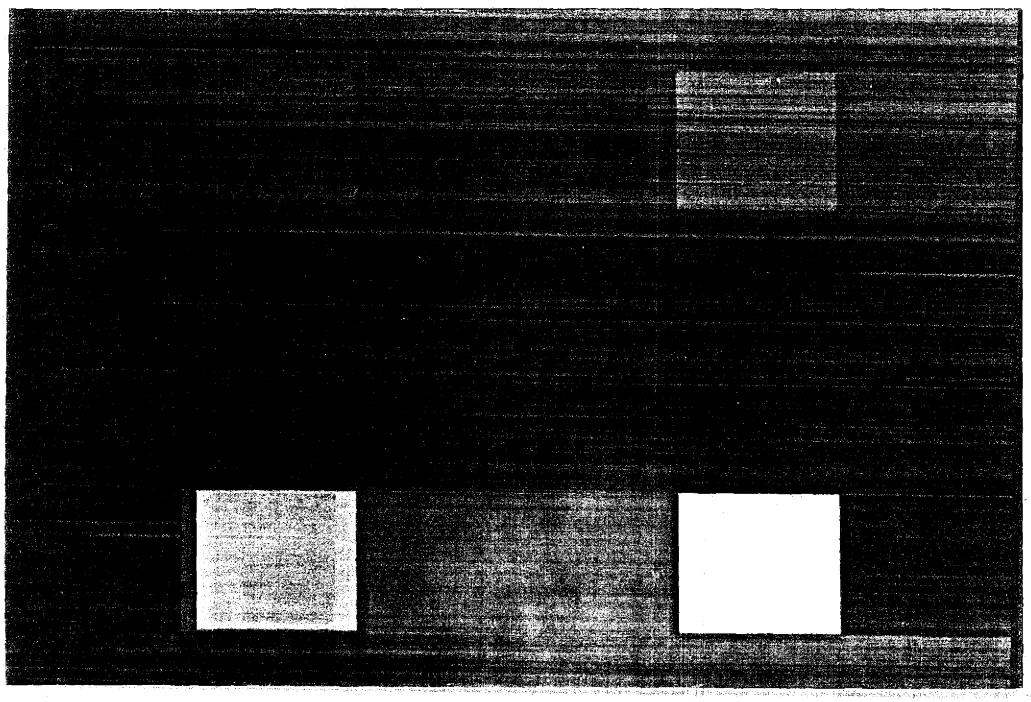

Figure 21. TEST1, Linear Filtering, SF=1

Figure 22. CMAN, Smoothed Gradient Picture

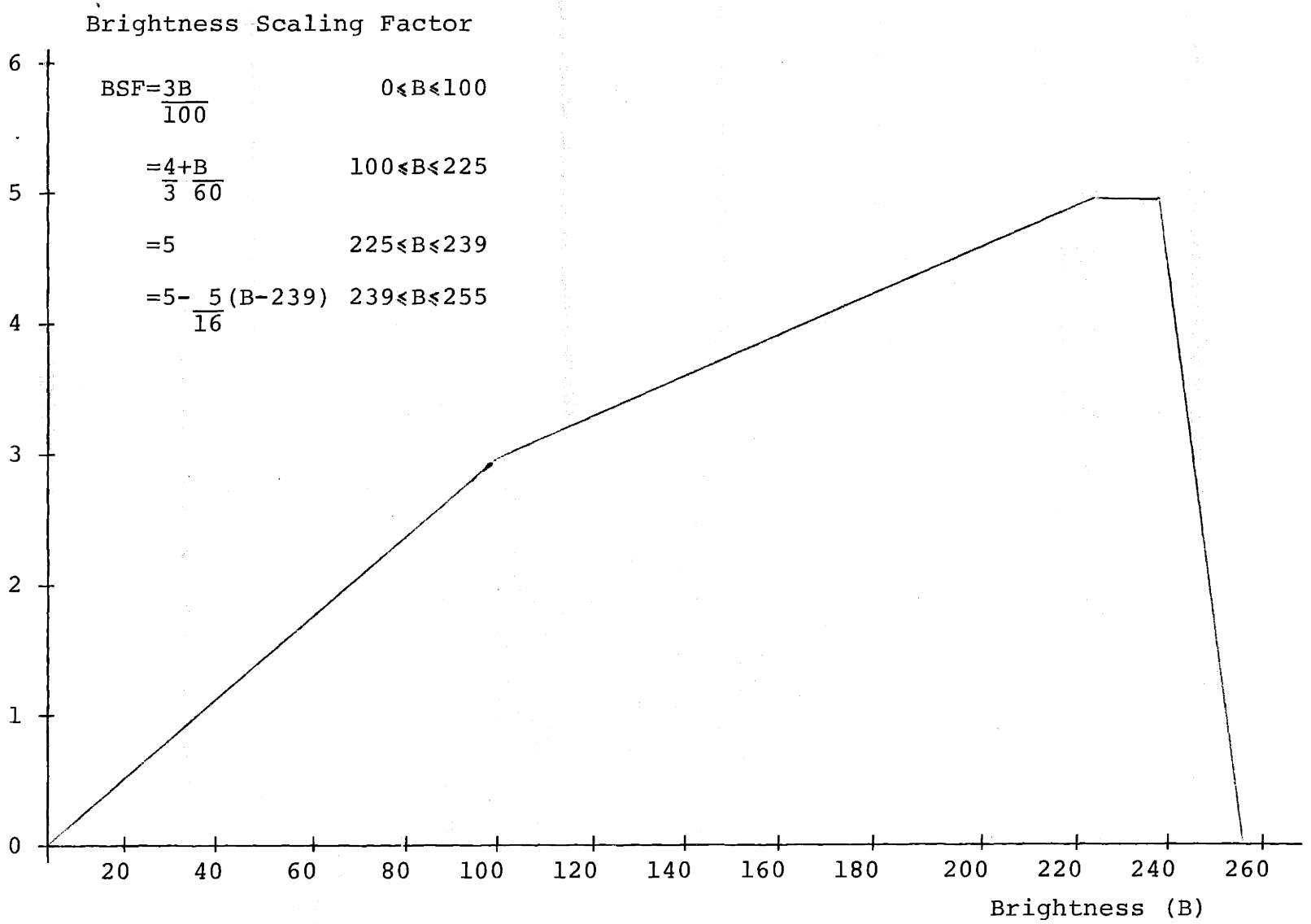

Figure 23. Brightness Scaling Function, 4 pel edge radius

Figure 25. CMAN, Equalized Adaptive Filtering, SF=15

Figure 26. CMAN, Gilkes Adaptive Filtering, SF=.8

Figure 27. CMAN, Homomorphic Filtering, dc gain=.875, ∞ gain=2

Figure 28. CMAN, Linear Filtering, SF=.4

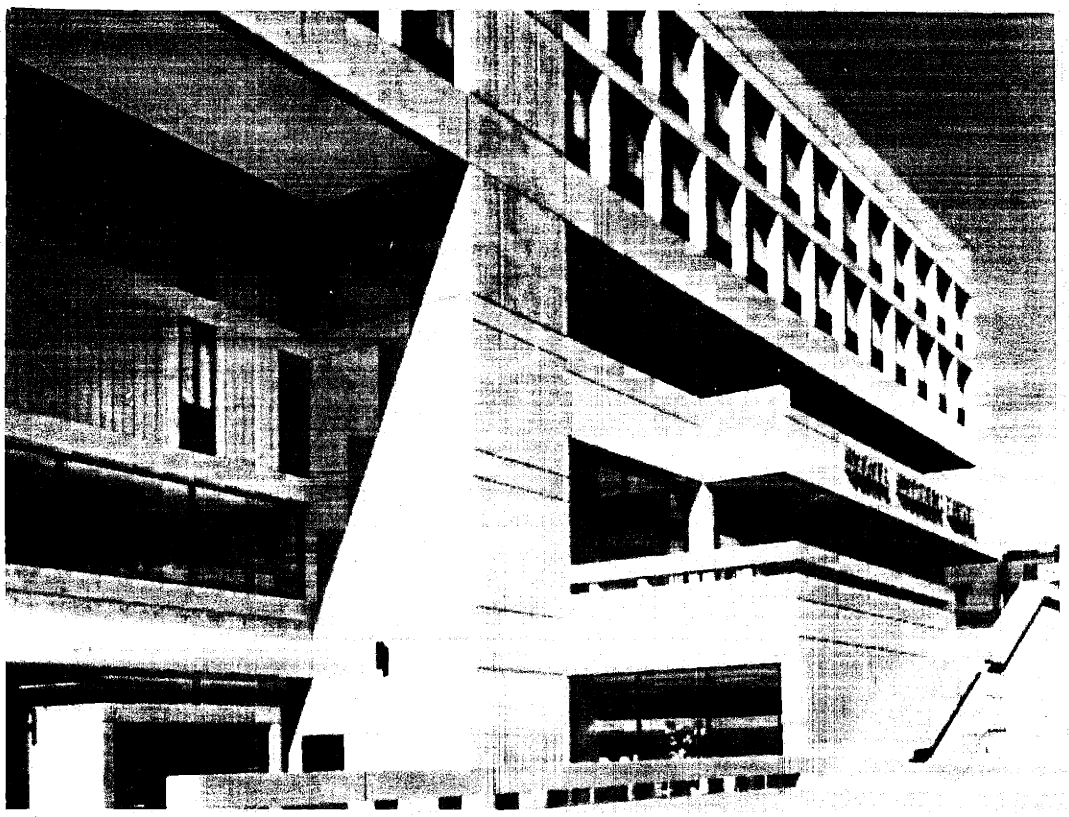

Figure 29. BANK, Original

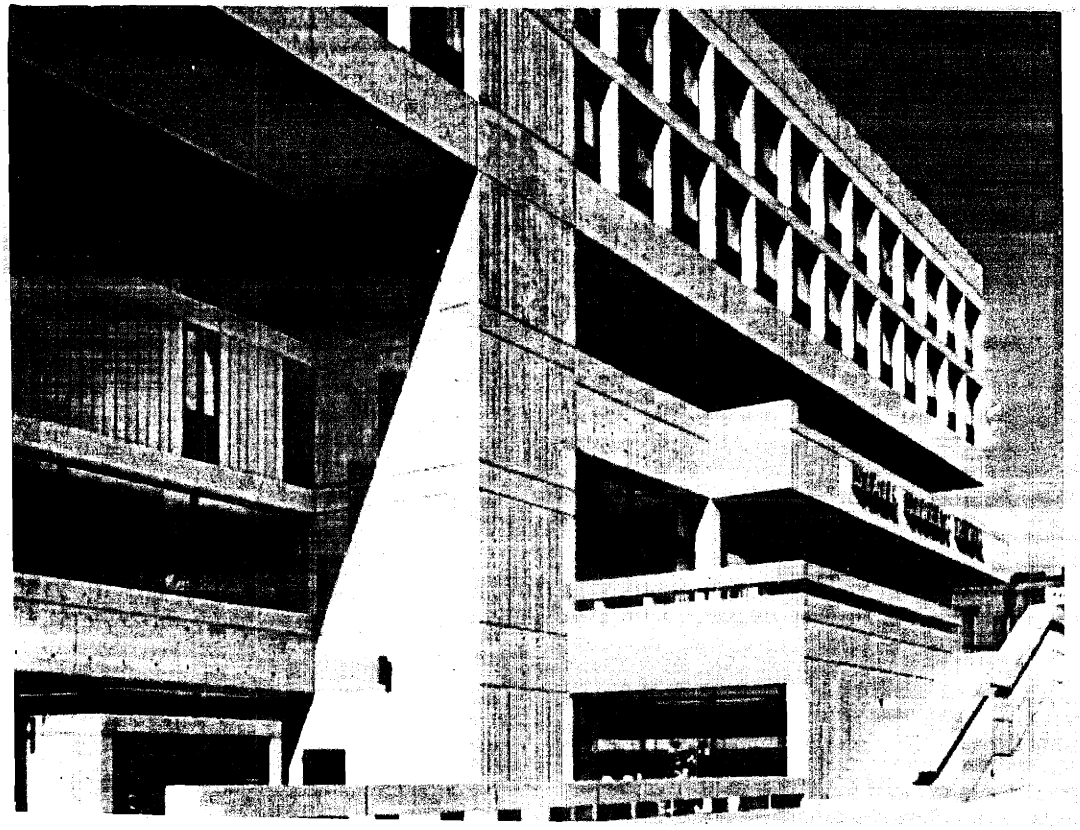

Figure 30. BANK, Equalized Adaptive Filtering, SF=12

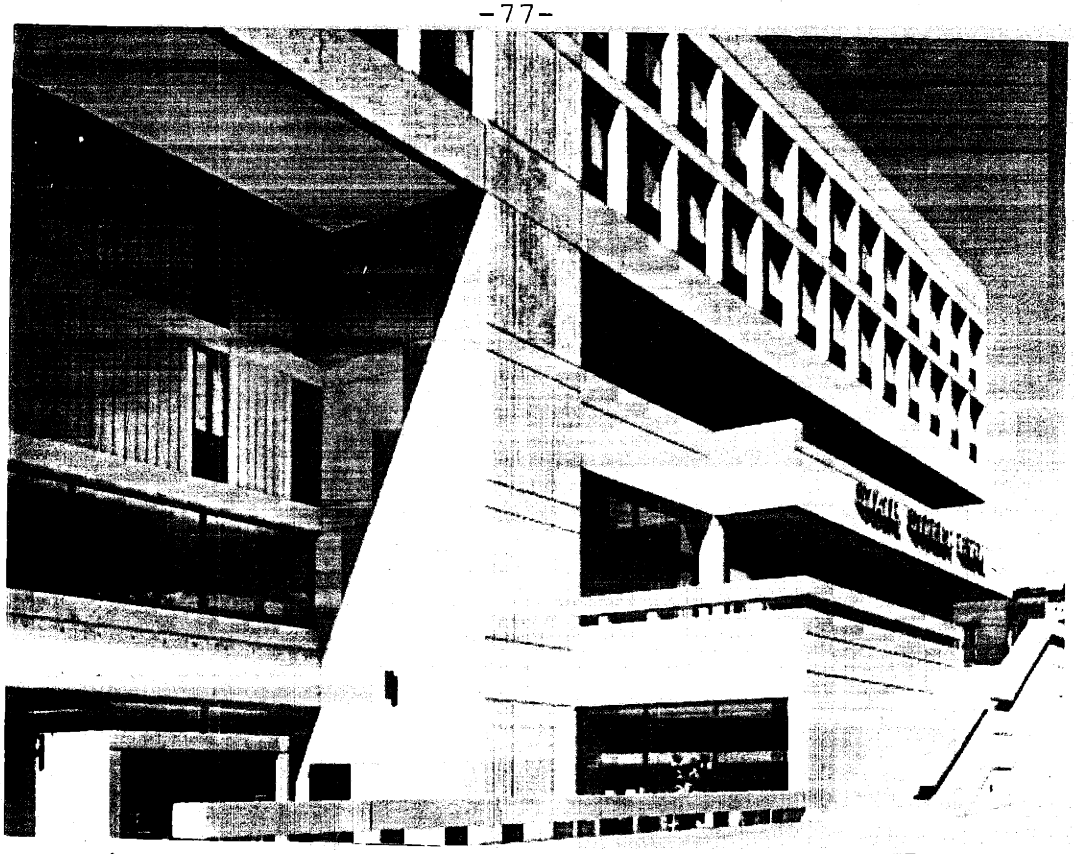

Figure 31. BANK, Gilkes Adaptive Filtering, SF=1

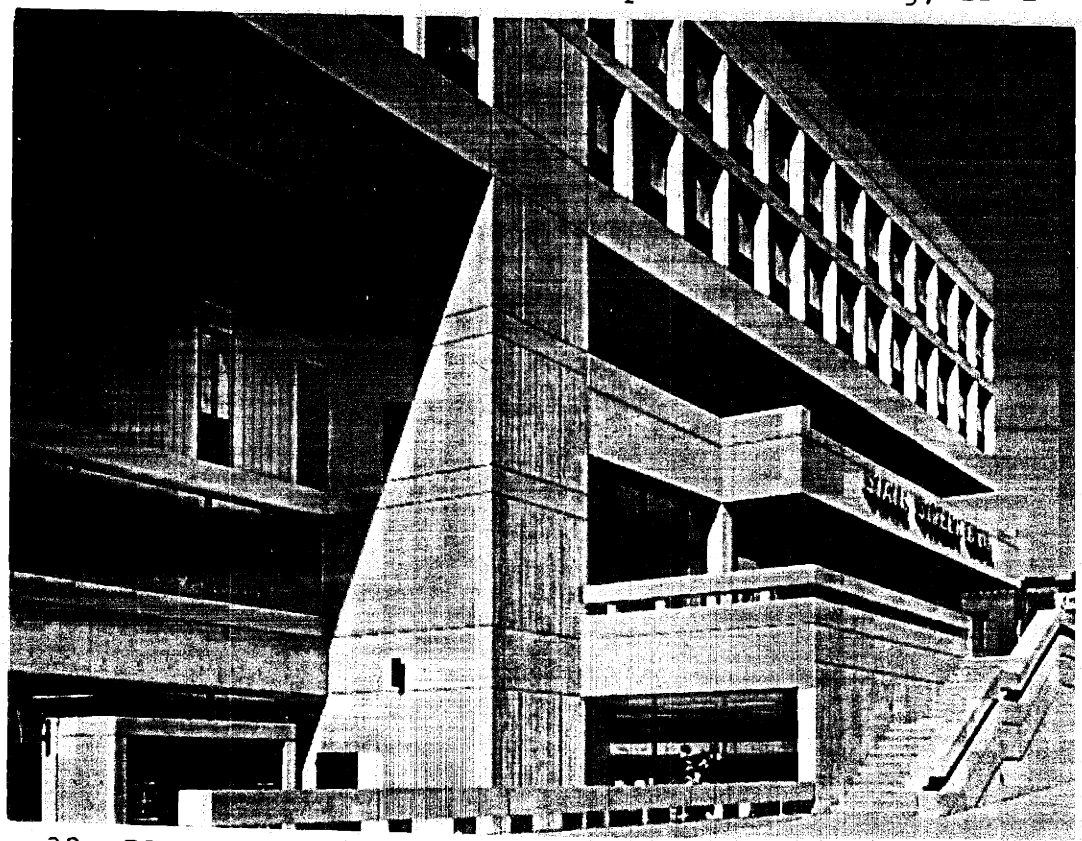

Figure 32. BANK, Homomorphic Filtering, dc gain=.875, gain=2

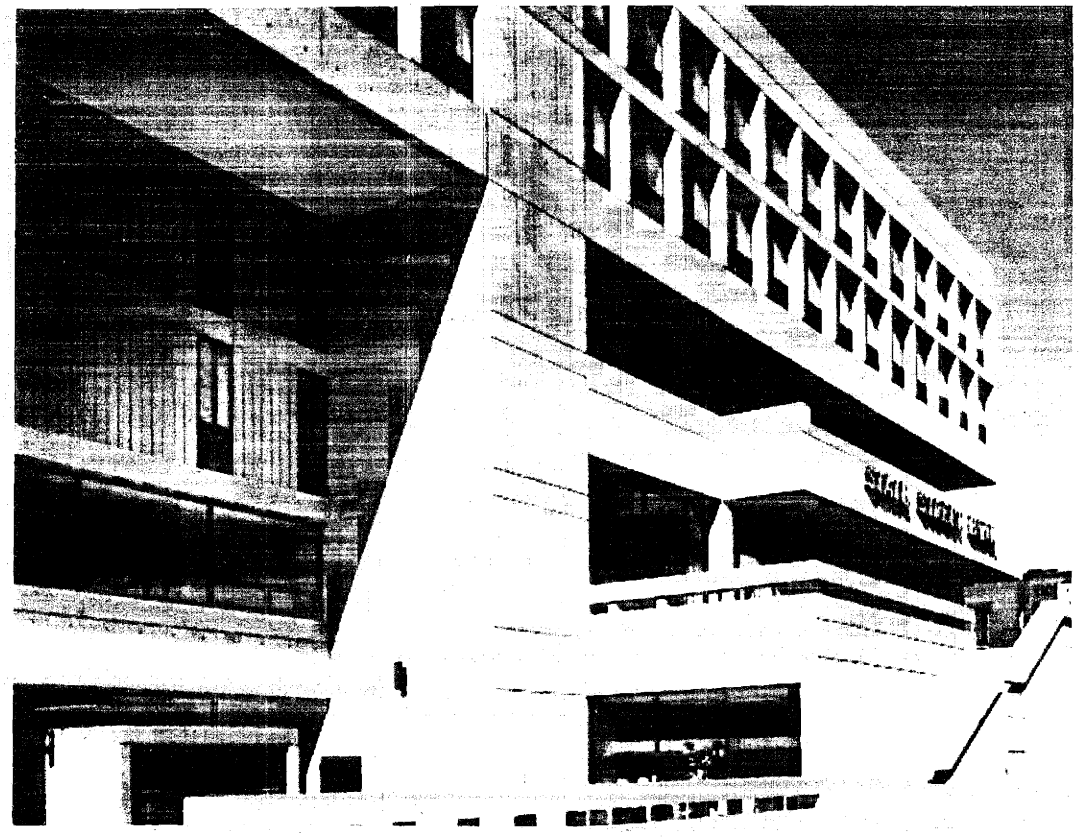

Figure 33. BANK, Linear Filtering, SF=.4

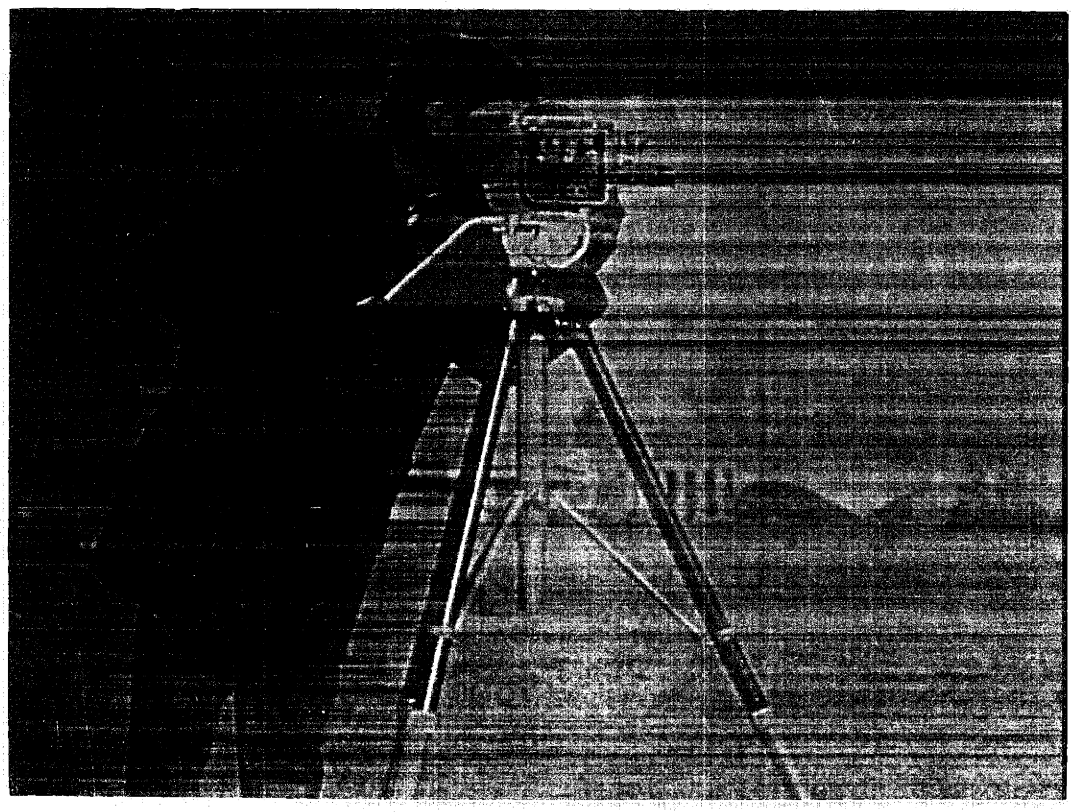

Figure 44. CMAN, Homomorphic Filtering, dc gain=.5, ∞ gain=2

Figure 34. DOC, Original

Figure 35. DOC, Equalized Adaptive Filtering, SF=10

Figure 36. DOC, Gilkes Adaptive Filtering, SF=1.4

Figure 37. DOC, Homomorphic Filtering, dc gain=.875, ∞ gain=2

Figure 38. DOC, Linear Filtering, SF=.6

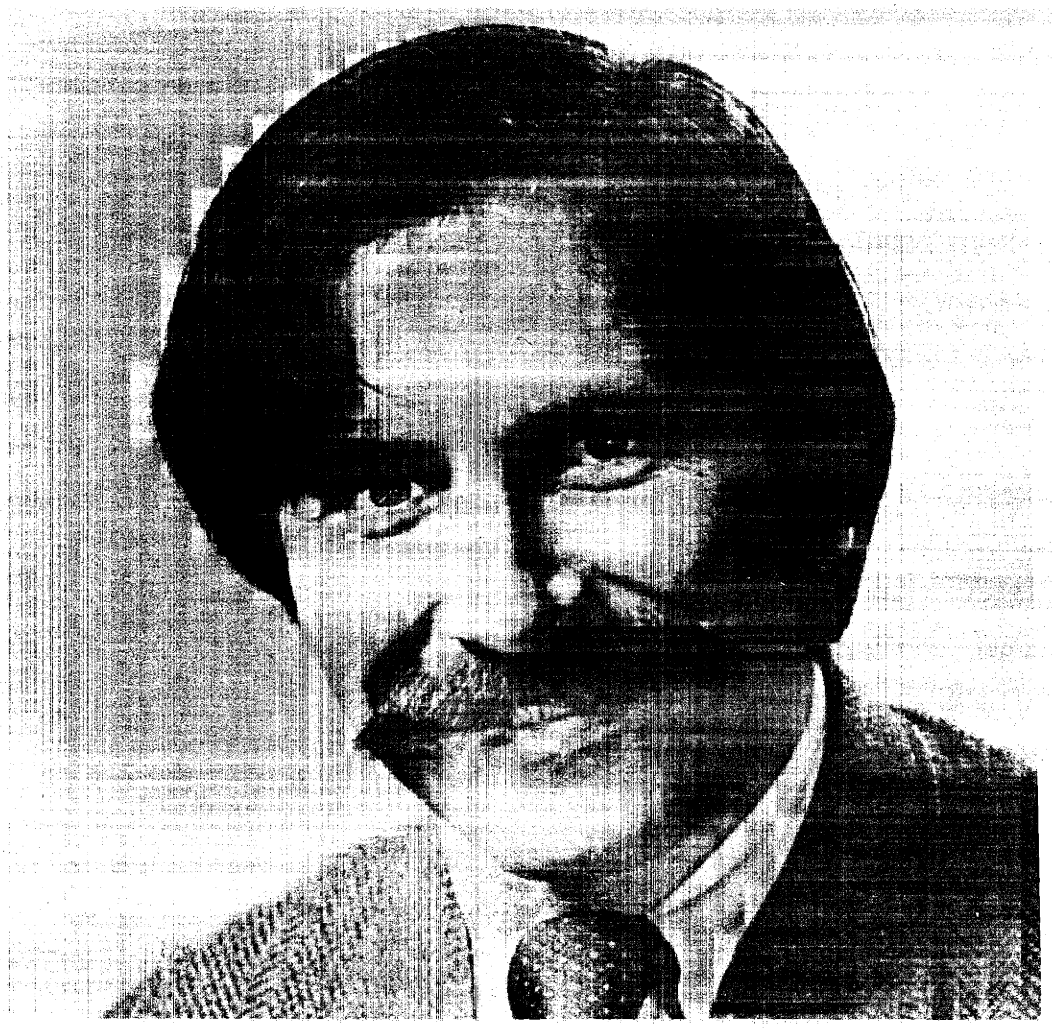

Figure 39. OLEH, Original

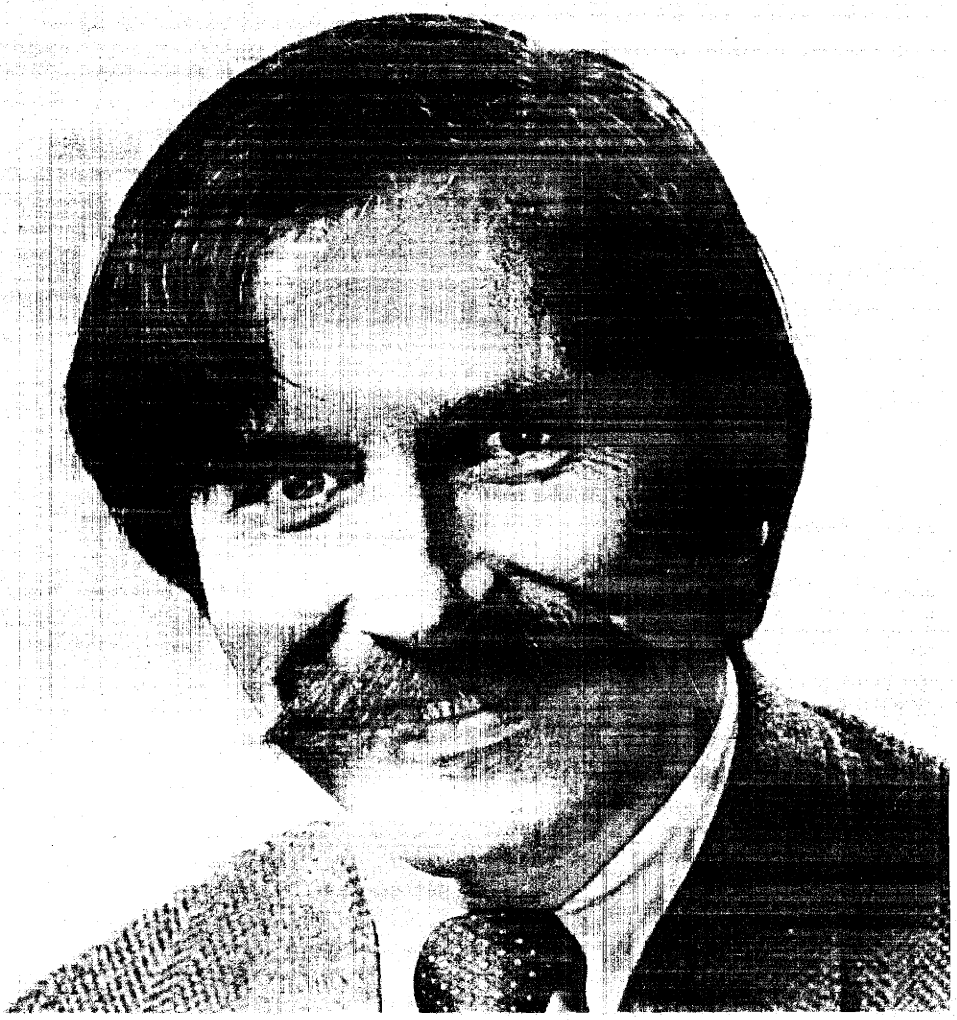

Figure 40. OLEH, Equalized Adaptive Filtering, SF=10

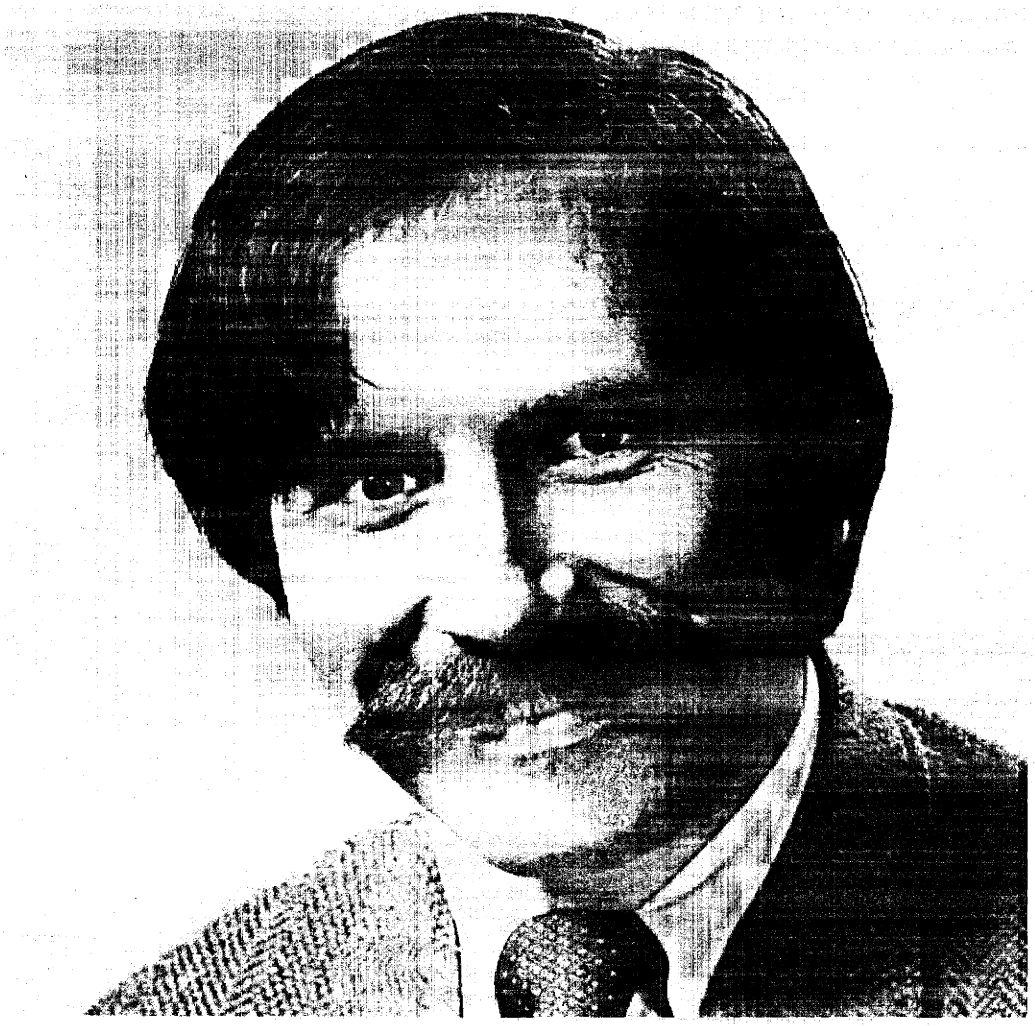

Figure 41. OLEH, Gilkes Adaptive Filtering, SF=1.2

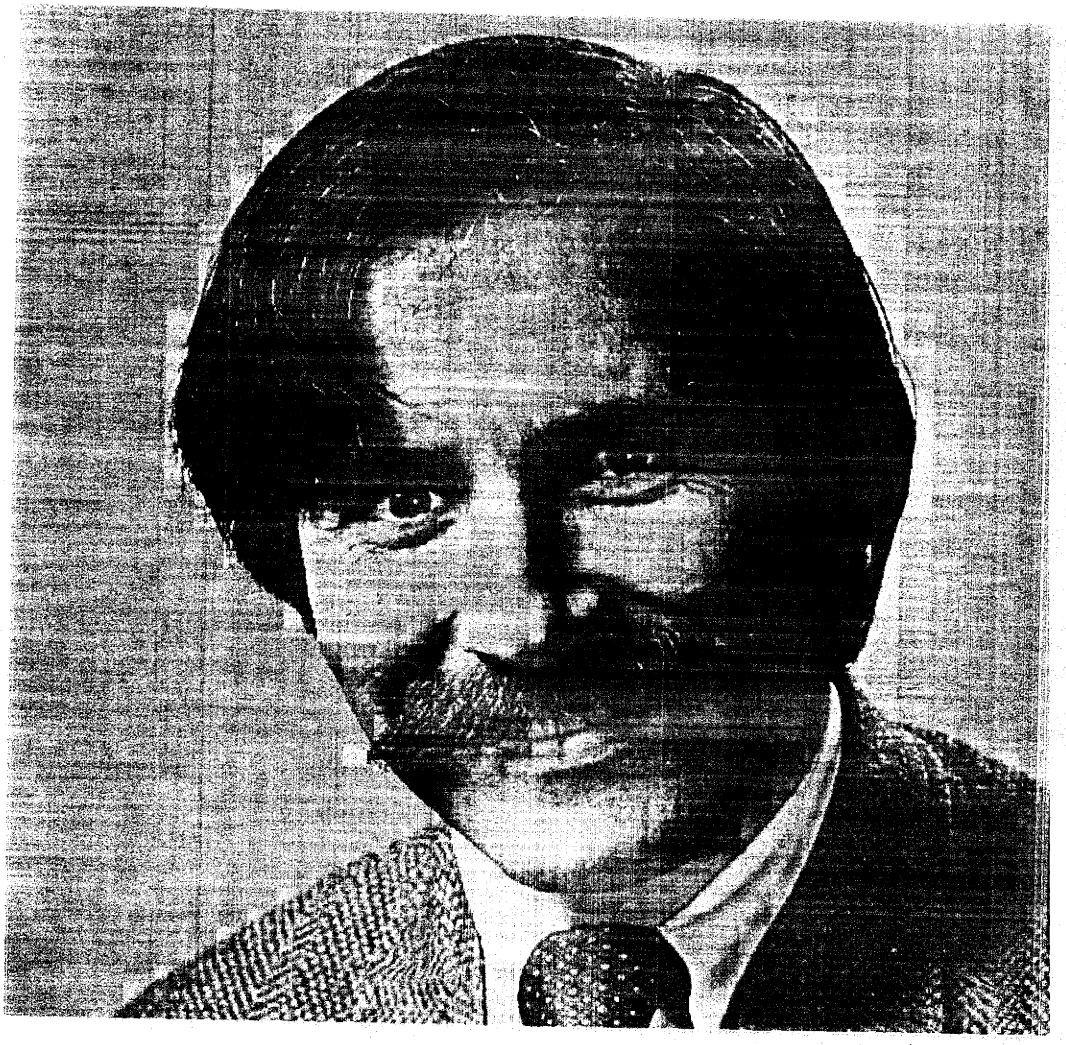

Figure 42. OLEH, Homomorphic Filtering, dc gain=.875, ∞ gain=2

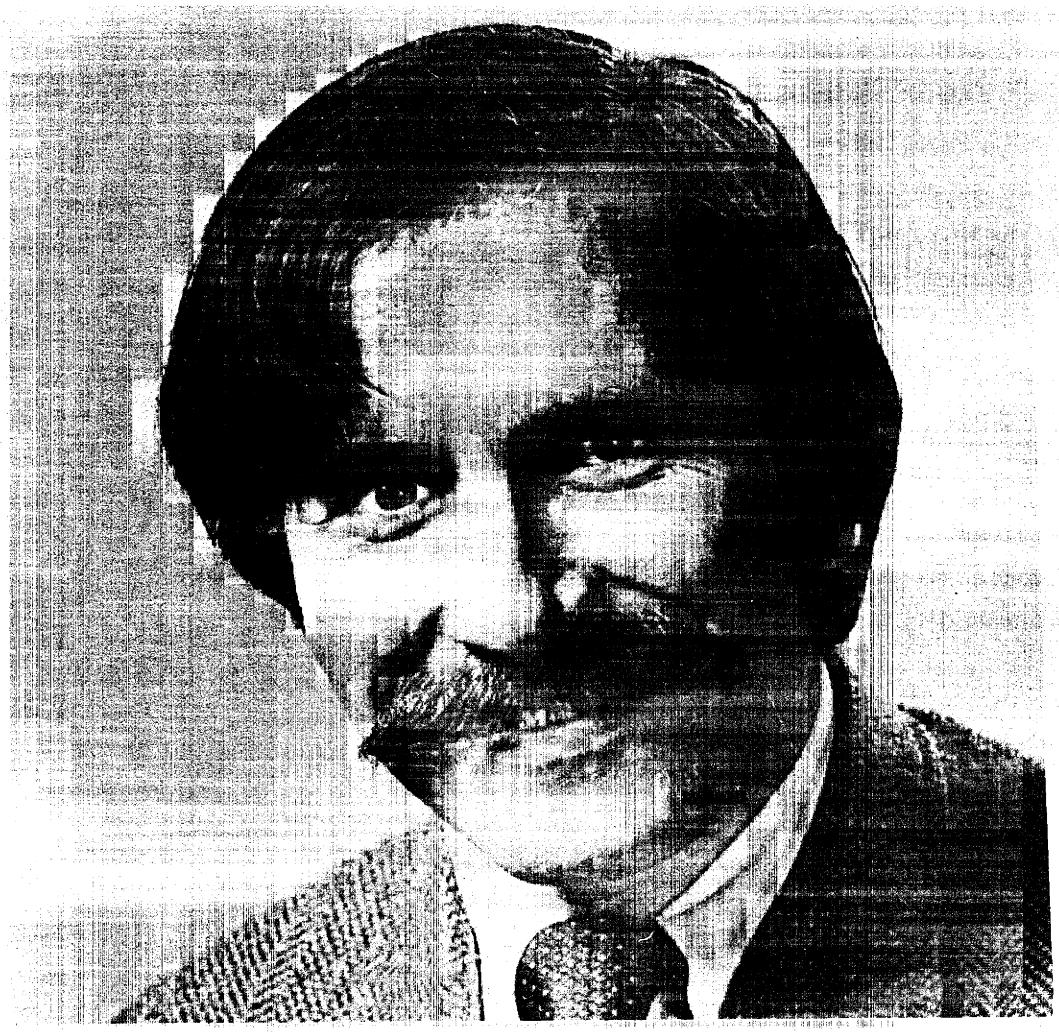

Figure 43. OLEH, Linear Filtering, SF=.5

Figure 45. CMAN, Quantized to 4 Bits, Noisy Picture

Figure 46. CMAN, Noise Suppressed, Enhanced Picture, SF=15

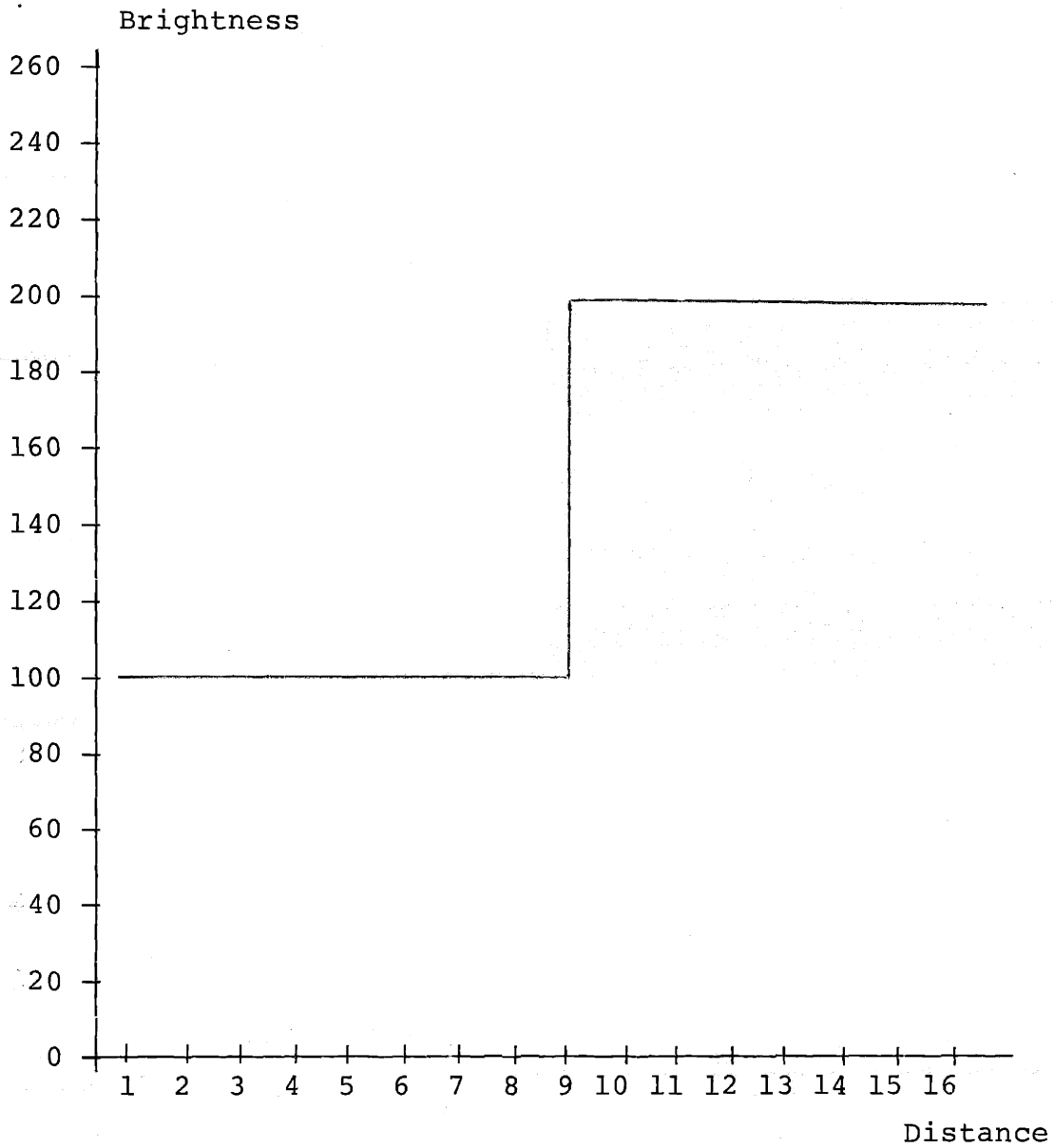

Figure 47. One Dimensional High Contrast Edge

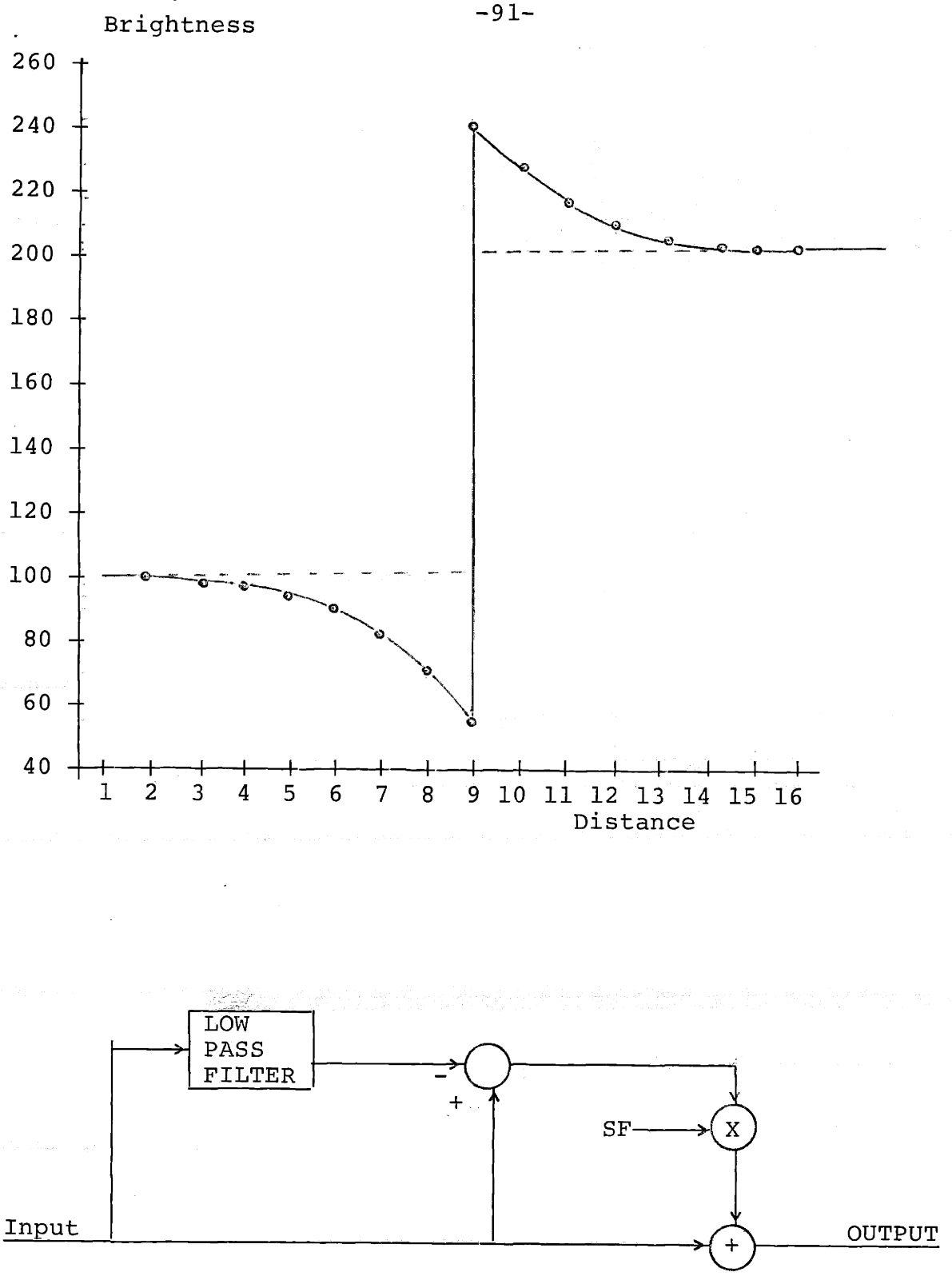

Figure 48. Linear Filtering Block Diagram and 1-D Edge

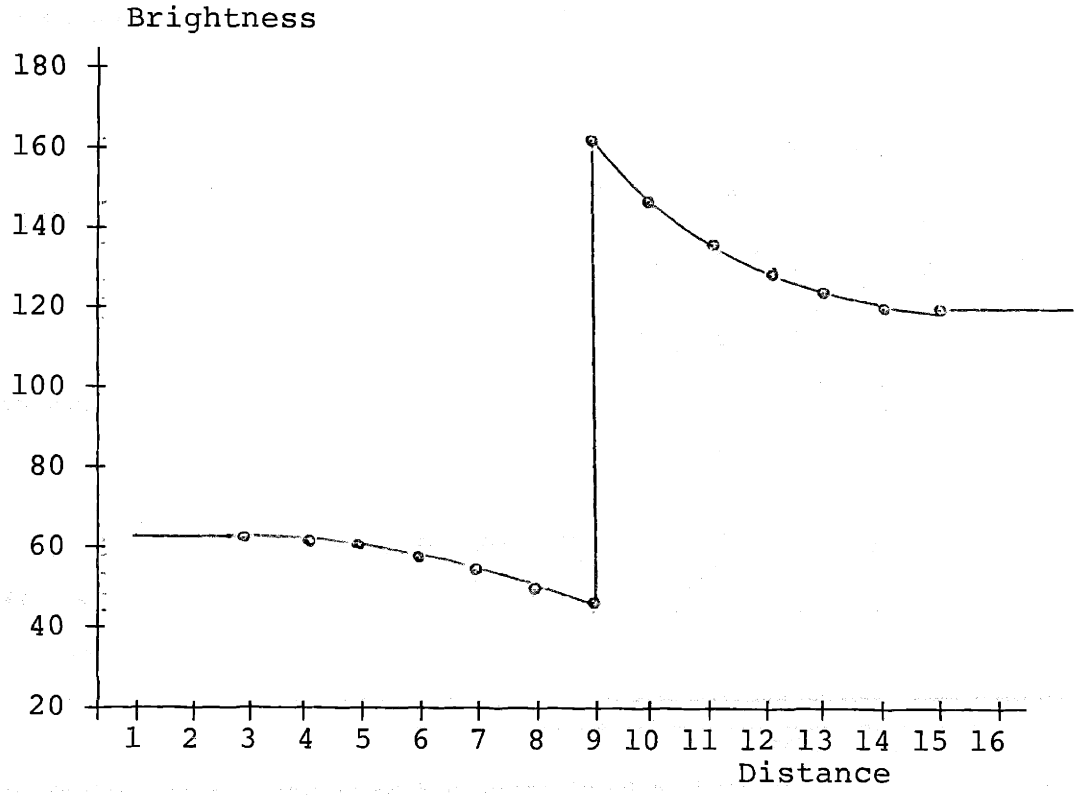

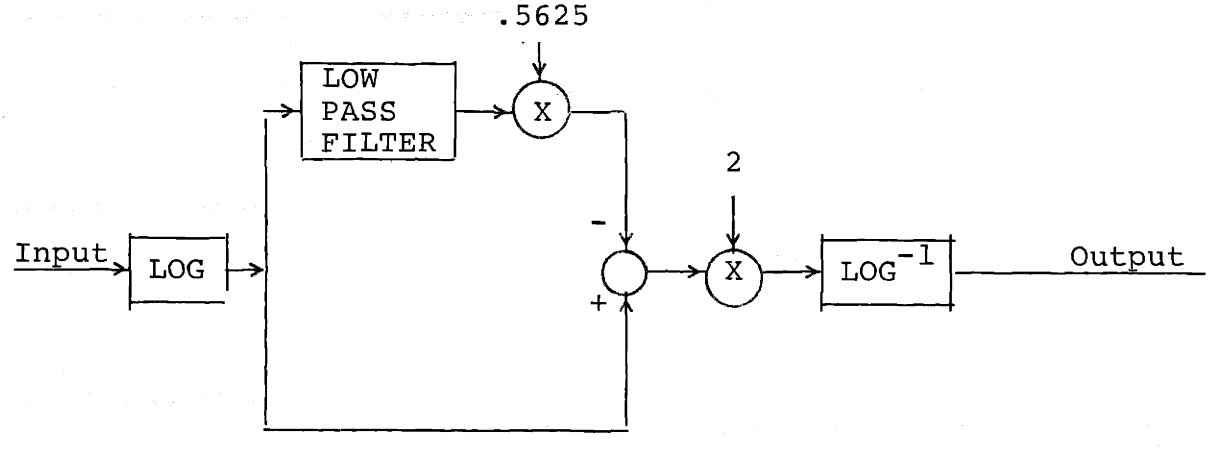

Figure 49. Homomorphic Filtering Block Diagram and 1-D Edge

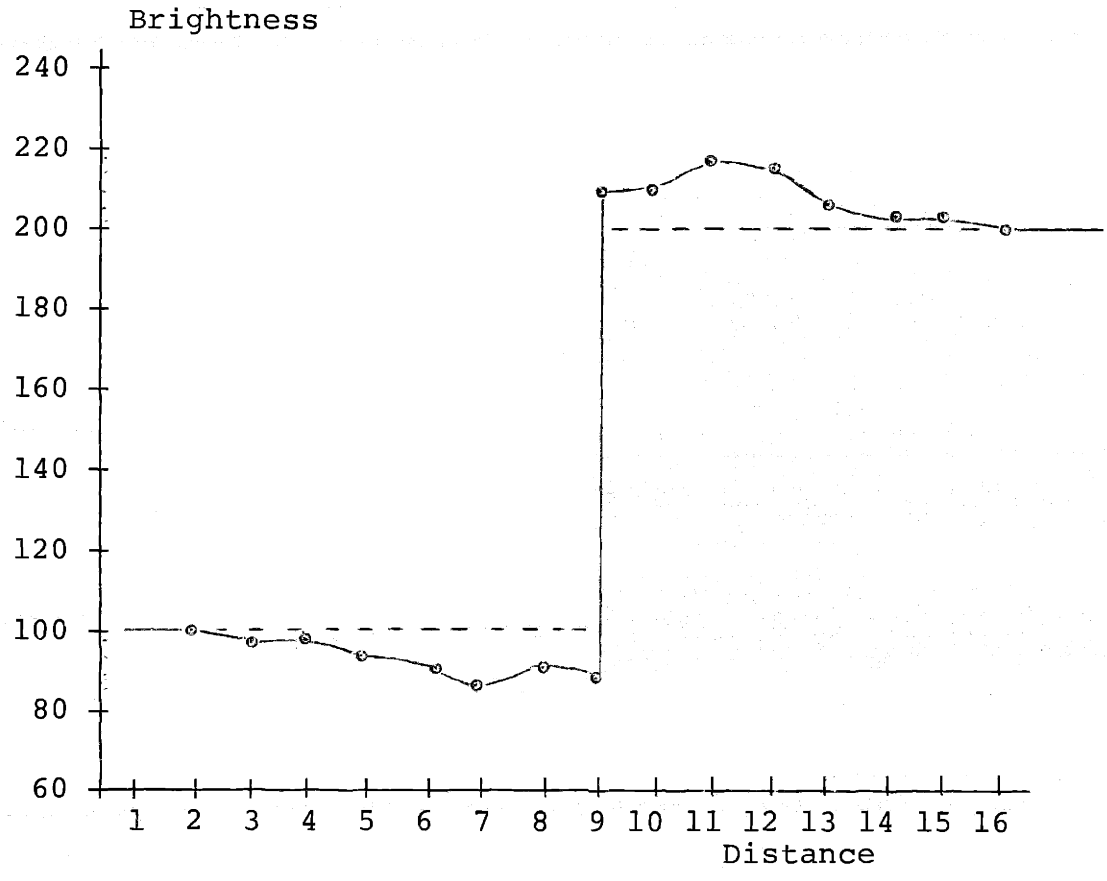

$$\text{Scaling Function} = .25 + 2.5 \frac{B_L}{256} \frac{g(32 - |B_E|, 0)}{32}$$

g(a,b)= greater of a and b

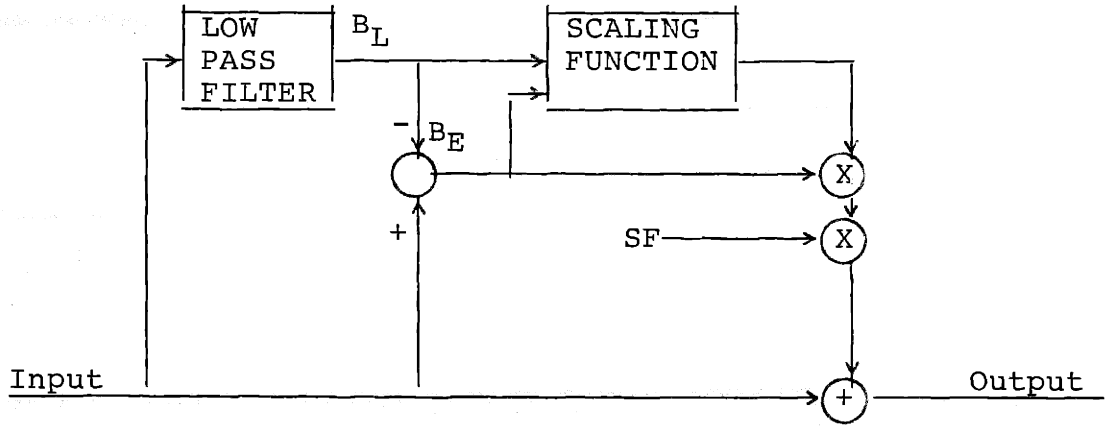

Figure 50. Gilkes Filtering Block Diagram and 1-D Edge

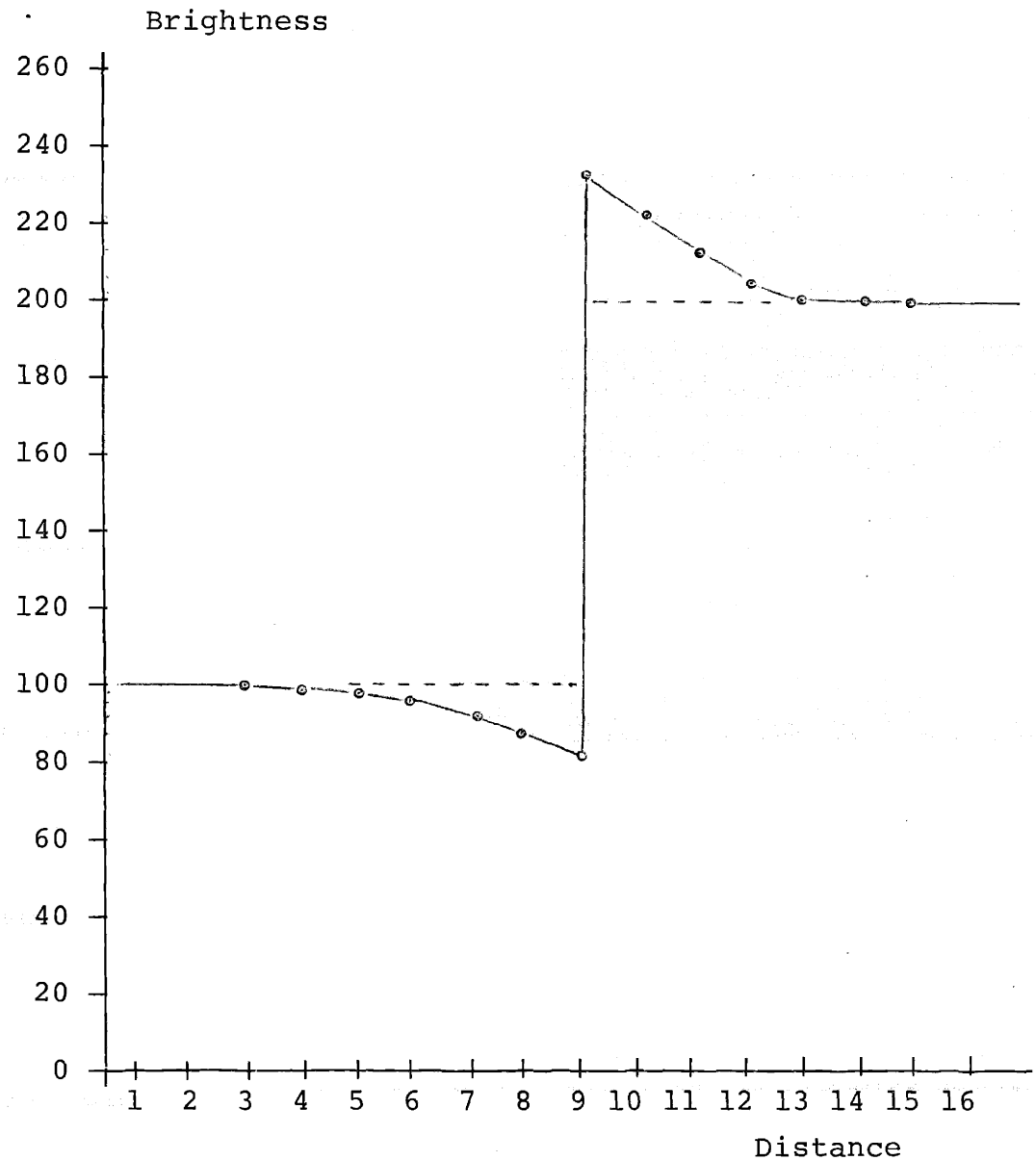

Figure 51. Equalized Adaptive Filtering, 8 pel edge radius

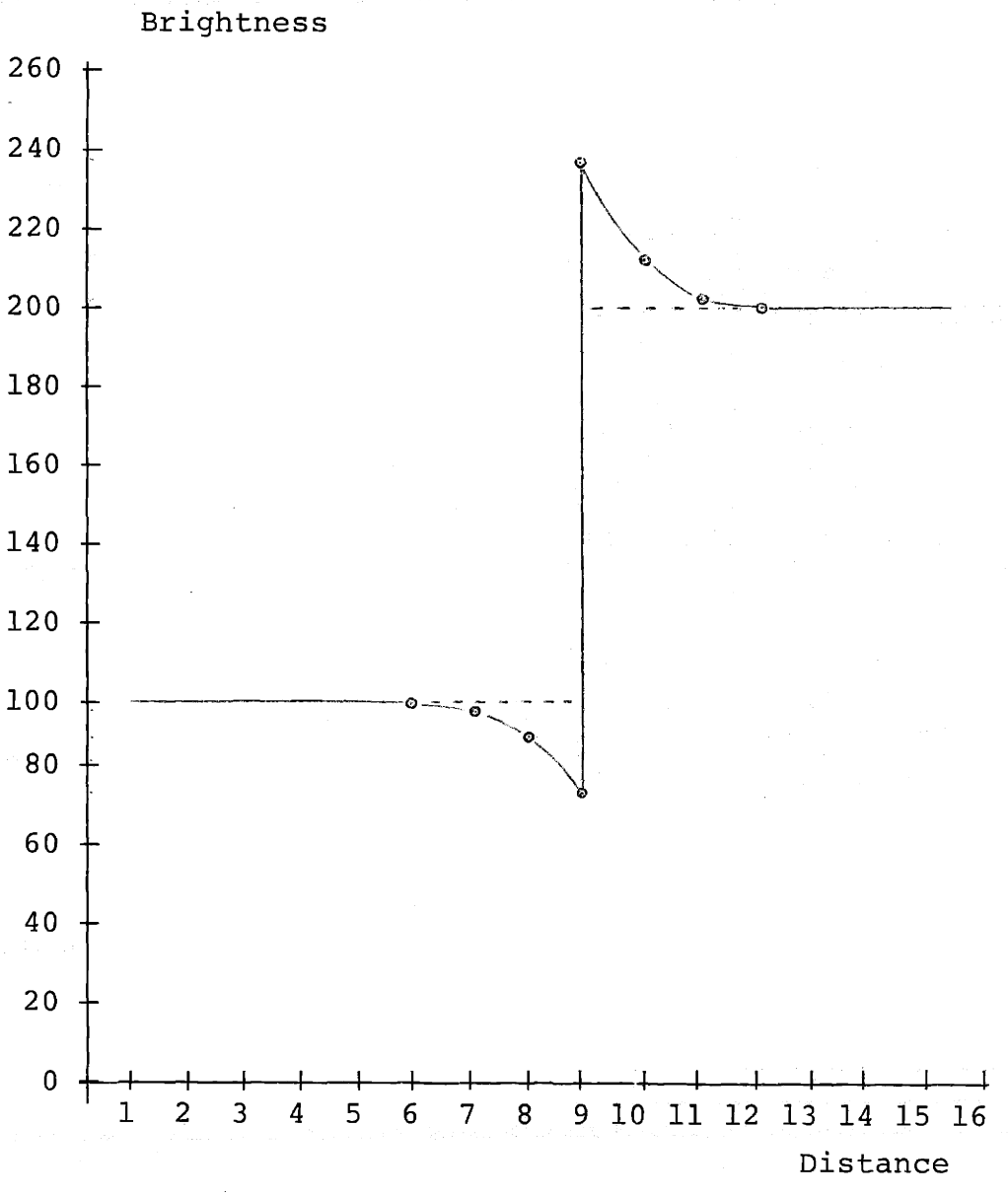

Figure 52. Equalized Adaptive Filtering, 4 pel edge radius

D=0	D=1	D=2	D=3	D=4	D=5	D=6	D=7	D=8	D=9
0	0	0	0	0	0	0	0	0	0
1	1	0	0	0	0	0	0	0	0
2	1	1	0	0	0	0	0	0	0
3	2	1	1	1	0	0	0	0	0
4	3	2	1	1	1	0	0	0	0
5	3	2	2	1	1	0	0	0	0
6	4	3	2	1	1	1	0	0	0
7	5	3	2	1	1	1	0	0	0
8	5	3	2	1	1	1	0	0	0
9	6	4	3	2	1	1	1	0	0
10	7	4	3	2	1	1	1	0	0
11	7	5	3	2	1	1	1	0	0
12	8	5	4	3	2	1	1	0	0
13	9	6	4	3	2	1	1	1	0
14	9	6	4	3	2	1	1	1	0
15	10	7	5	3	2	1	1	1	0
16	10	7	5	3	2	1	1	1	0
17	11	8	5	3	2	1	1	1	0
18	12	8	5	4	3	2	1	1	0
19	13	9	6	4	3	2	1	1	1
20	13	9	6	4	3	2	1	1	1
21	14	9	6	4	3	2	1	1	1
22	15	10	7	4	3	2	1	1	1
23	15	10	7	5	3	2	1	1	1
24	16	11	7	5	3	2	1	1	1
25	17	11	8	5	3	2	2	1	1
26	17	12	8	5	3	2	2	1	1
27	18	12	8	5	3	2	2	1	1
28	19	13	8	6	4	3	2	1	1
29	19	13	9	6	4	3	2	1	1
30	20	13	9	6	4	3	2	1	1

Figure 53. Exponential Edge Shapes

Overshoot=exp(-D/2.5)

BRIGHTNESS		SUBJECTS									SMOOTHING			
Stripe	Backgr.	1	2	3	4	5	6	7	8	Averg.	1	2	3	4
20	25	3	4	2	5	3	2	3	3	3.00	3.33	3.52	3.57	3.61
40	45	4	4	2	5	4	4	4	4	4.00	3.89	3.67	3.68	3.69
60	65	4	4	4	8	4	6	4	6	4.67	3.78	3.85	3.83	3.87
80	85	2	2	2	6	2	2	4	4	2.67	3.89	3.96	4.10	4.14
100	105	3	3	5	7	3	5	5	5	4.33	4.22	4.48	4.50	4.54
120	125	2.5	7	5	9	5	5	5	7	5.67	5.33	5.07	5.01	4.94
145	150	4	8	4	8	8	4	4	8	6.00	5.66	5.48	5.32	5.23
170	175	4	8	4	14	4	4	4	8	5.33	5.44	5.40	5.37	5.32
210	215	5	5	2	8	5	5	5	5	5.00	5.11	5.22	5.28	5.31

Figure 54. Subjective Testing Results, Overshoot versus Brightness

BRIGHTNESS Stripe	Backgr.	SUBJECTS 1	2	3	4	5	6	7	8	Averg.	SMOOTH 1	Smoothed Oversht. Backgr.
60	65	4	4	4	8	4	4	4	6	4.33	3.72	.0572
60	70	2	2	1	2	2	5	2	5	2.50	4.00	.0571
60	75	2	4	4	7	7	7	4	10	5.17	5.22	.0696
60	80	3	9	3	9	12	9	6	15	8.00	8.06	.1008
60	90	7	13	7	10	13	10	13	16	11.00	10.00	.1111
100	105	3	3	5	7	3	5	5	5	4.50	5.17	.0492
90	100	8	5	3	10	8	3	12	5	6.50	5.61	.0561
90	105	9	4	4	6	6	4	9	6	5.83	6.55	.0624
90	110	7	9	7	7	7	7	7	9	7.33	7.61	.0692
90	120	8	12	6	12	12	6	16	8	9.67	8.89	.0741
145	150	4	8	4	8	8	4	4	8	6.00	5.78	.0385
145	155	4	8	4	13	4	4	4	8	5.33	6.69	.0432
145	160	5.5	14	5.5	14	5.5	11	5.5	11	8.75	7.61	.0476
145	165	5.5	14	5.5	17	11	5.5	5.5	11	8.75	9.93	.0602
145	175	6	15	12	15	15	15	12	15	12.30	11.12	.0635
170	175	4	8	4	14	4	4	4	8	3.75	4.61	.0263
175	185	4	8	8	10	4	4	8	6	6.33	6.03	.0326
175	190	10	8	8	6	10	6	10	6	8.00	7.72	.0406
175	195	11	9	12	11	11	7	13	9	8.83	8.83	.0453
175	205	12	6	15	12	12	8	8	6	9.66	9.38	.0458

Figure 55. Subjective Testing Results, Overshoot versus Contrast

BIBLIOGRAPHY

1. C.W. Helstrom, "Image Restoration by the Method of Least Squares," J.O.S.A., vol. 57, pp. 297-303, March 1967.

2. A.A. Sawchuk, "Space Variant Image Motion Degradation and Restoration," Proc. IEEE.,vol.60, no. 7, pp.854-861, July 1972.

3. G.M. Robbins, T.S. Huang, "Inverse Filtering for Linear Shift-Variant Imaging Systems," Proc. IEEE, vol. 60, no. 7, pp. 862-872, July 1972.

4. T.S. Huang, W.F. Schreiber, O.J. Tretiak, "Image Processing," Proc. IEEE, vol. 59, pp. 1586-1609, Nov. 1971.

5. R.M. Evans, An Introduction to Color, New York, John Wiley and Sons, 1948.

6. W.F. Schreiber, "Picture Coding," Proc. IEEE, vol. 55, no. 3, March 1967.

7. W.F. Schreiber, C.F. Knapp, "TV Bandwidth Reduction by Digital Signal Coding," IRE National Convention Record, pt. 4, pp. 88-100, 1958.

8. C.E.K. Mees, T.H. James, eds., The Theory of the Photographic Process, Third Edition, New York: Macmillan Co., 1966.

9. T.N. Cornsweet, Visual Perception, New York: Academic Press, 1970.

10. U. Malone, "New Data on Noise Visibility," MS Thesis, MIT, Department of Electrical Engineering, 1977.

11. B. Hashizume, "Companding in Image Processing," BS Thesis MIT, Department of Electrical Engineering, 1973.

12. L.G. Roberts, "Picture Coding Using Pseudo-Random Noise," IRE Transactions on Information Theory, vol. IT-8, pp. 145-154, Feb. 1962.

13. O.W. Mitchell, "The Effect of Spatial Frequency on the Visibility of Unstructured Patterns," Ph.D. Thesis, MIT, Department of Electircal Engineering, 1972.

14. W.F. Schreiber, "Wirephoto Quality Improvement by Unsharp Masking," Pattern Recognition, vol. 2, no. 2, pp. 117-121, May 1970.

15. A.V. Oppenheim, R.W. Schafer, T.G. Stockham, "Non-Linear Filtering of Multiplied and Convoled Signals," Proc. IEEE, vol. 56, pp. 1264-1291, Aug. 1968.

16. T.G. Stockham, "Image Processing in the Context of a Visual Model," Proc. IEEE, vol. 60, no. 7, pp.828-842, July 1972.

17. W.F. Schreiber, "Image Processing for Quality Improvement," unpublished, March 1977.

18. A.M. Gilkes, "Photographic Enhancement by Adaptive Digital Unsharp Masking,"MS Thesis, MIT, Department of Electrical Engineering, 1977.

19. V. O'Brien, "Contour Perception, Illusion and Reality," J.O.S.A., vol. 48, no. 2, pp. 112-119, Feb. 1958.

20. CIPG Picture Processing System Operator's Manual, MIT, Sept. 1976.

21. D. Wood, "Histogram Based Adaptive Quantizing," MS Thesis, MIT, Department of Electrical Engineering, August 1977.